AD-A140 912 DEVELOPMENT OF HIGH MODULUS POLYDIACETYLENE FIBRES FOR USE IN FIBRE-REINF..(U) QUEEN MARY COLL LONDON (ENGLAND) DEPT OF MATERIALS R J YOUNG ET AL. FEB 84 1/1

UNCLASSIFIED DAJA37-81-C-0501 F/G 11/9 NL

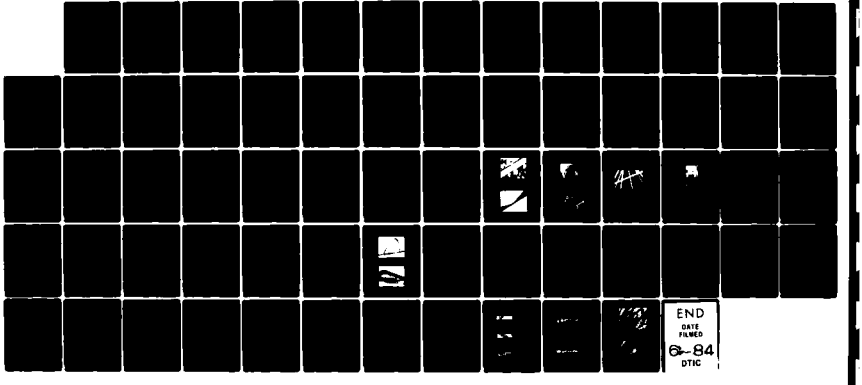

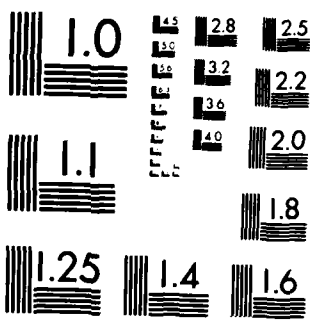

DEVELOPMENT OF HIGH MODULUS POLYDIACETYLENE FIBRES FOR USE IN FIBRE-REINFORCED COMPOSITES

FINAL TECHNICAL REPORT

by

R.J. Young, C. Galiotis and P.H.J. Yeung

February 1984

UNITED STATES ARMY

EUROPEAN RESEARCH OFFICE OF THE U.S. ARMY

London England

Contract Number : DAJA37-81-C-9501

Materials Department
Queen Mary College
(University of London)

Approved for Public Release; distribution unlimited

UNCLASSIFIED

SECURITY CLASSIFICATION OF THIS PAGE (When Data Entered)

R&D 2840-MS

REPORT DOCUMENTATION PAGE	READ INSTRUCTIONS BEFORE COMPLETING FORM
1. REPORT NUMBER / 2. GOVT ACCESSION NO. AD-A140 912	3. RECIPIENT'S CATALOG NUMBER
4. TITLE (and Subtitle) Development of High Modulus Polydiacetylene Fibres for Use in Fibre-Reinforced Composites	5. TYPE OF REPORT & PERIOD COVERED Final Technical Report
	6. PERFORMING ORG. REPORT NUMBER
7. AUTHOR(s) R. J. Young, C. Galiotis, P.H.J. Yeung	8. CONTRACT OR GRANT NUMBER(s) DAJA37-81-C-0501
9. PERFORMING ORGANIZATION NAME AND ADDRESS Queen Mary College, University of London	10. PROGRAM ELEMENT, PROJECT, TASK AREA & WORK UNIT NUMBERS 6.11.02A IT161102BH57-04
11. CONTROLLING OFFICE NAME AND ADDRESS USARDSG-UK Box 65, FPO NY 09510	12. REPORT DATE February 1984
	13. NUMBER OF PAGES 61
14. MONITORING AGENCY NAME & ADDRESS(if different from Controlling Office)	15. SECURITY CLASS. (of this report) Unclassified
	15a. DECLASSIFICATION/DOWNGRADING SCHEDULE

16. DISTRIBUTION STATEMENT (of this Report)

Approved for public release: distribution unlimited

17. DISTRIBUTION STATEMENT (of the abstract entered in Block 20, if different from Report)

18. SUPPLEMENTARY NOTES

19. KEY WORDS (Continue on reverse side if necessary and identify by block number)

Polydiacetylenes, mechanical properties, composites, structure, electron microscopy, fracture, Raman spectroscopy

20. ABSTRACT (Continue on reverse side if necessary and identify by block number)

The relationship between structure and mechanical properties in polydiacetylene single crystal fibres has been studied in detail. It has been shown by transmission electron microscopy that the fibres have a high degree of internal perfection with the polymer molecules aligned parallel to the fibre axes. The fibres of the di-carbazolyl derivative investigated were found to have a Young's modulus of 45 GPa and fracture strengths of up to 1.5 GPa, the strength being controlled by defects such as surface steps.

DD FORM 1 JAN 73 1473 EDITION OF 1 NOV 65 IS OBSOLETE

UNCLASSIFIED

SECURITY CLASSIFICATION OF THIS PAGE (When Data Entered)

It was shown that the stiffness of the polymer backbone is similar to that of polyethylene and the theoretical strength of the polydiacetylene single crystal fibres has been determined to be about 3 GPa, corresponding to a fracture strain of between 6% and 8% and a force required to break molecules of the order of 3nN. The derivative studied was also found to have good thermal stability, not degrading below 300°C, and excellent creep resistance up to at least 100°C.

A model composite system consisting of one polydiacetylene single crystal fibre in an epoxy resin matrix has been subjected to tensile strain parallel to the fibre direction. The strain at all points along the length of the fibre was determined by resonance Raman spectroscopy while that of the matrix was measured by conventional techniques. Comparison of the fibre and matrix strain showed two distinct regions. Below about 0.5% matrix strain the composite followed Reuss type behavior with equal stress in the fibre and the matrix. At higher matrix strain the composite followed Voigt type behaviour with any increase in matrix strain matched by an equal increase in fibre strain. In this region the strain distribution along the length of the fibre could be approximately described by the shear-lag model of Cox. The critical length of the fibre was found to increase linearly with fibre diameter as predicted by that model. Good qualitative agreement was found with the predictions of a calculation based on finite element analysis over the full range of applied stress.

The resonance Raman strain measurement technique has been extended to measure the distribution of fibre strain in composites containing bundles of polydiacetylenes in both an epoxy matrix and a glass-fibre/epoxy/ composite. It has been found that at low volume fractions the strain in the individual fibres is less than that in the matrix as for the single fibre model composite whereas when the fibre volume fraction exceeds about 8% the strain in the fibres and matrix are similar.

Finally, the deformation of epoxy composites containing high volume fractions of polydiacetylene single crystal fibres has been investigated in both tension and compression. Strengths of up to 150 MPa for composites with over 50% by volume of fibres have been measured in tension and this is about twice the compressive strength of similar composites. Failure in compression occurs by local buckling of the composite bar whereas fibre pull-out and fibre fracture take place during tensile deformation.

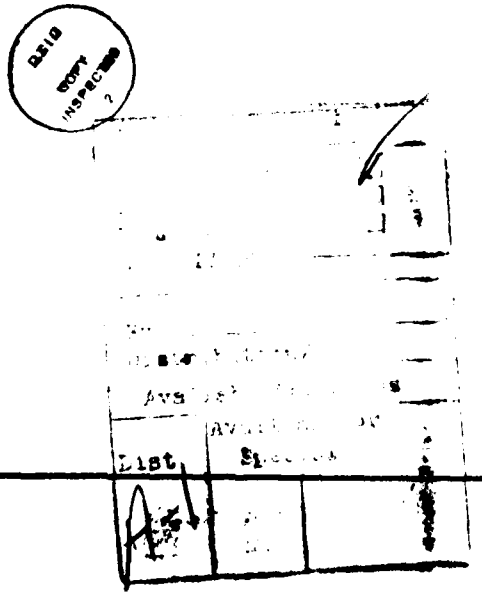

CONTENTS

1. INTRODUCTION

This report covers the period July 1981 to December 1983 of the project concerned with the development of polydiacetylene single crystal fibres and their use in fibre-reinforced composites. It is broken down into three main sections.

The first (section 2) describes the relationship between the structure and mechanical properties of polydiacetylene single crystal fibres. It is demonstrated that the unique single crystal fibres have perfect molecular alignment and a high degree of structural perfection. This leads to the crystals having a high value of Young's modulus which depends only upon the size of the side-group on the polymer backbone. The strength of the crystals is demonstrated to be controlled by surface defects and this allows the strength of the individual molecules to be determined. Creep and the general deformation of the fibres is also investigated.

In the next section (3) the use of resonance Raman spectroscopy to measure the distribution of fibre strain in a single-fibre model composite is demonstrated. This allows both the fundamental mechanisms of fibre reinforcement and the efficiency of stress transfer in the polydiacetylene/epoxy composite system to be investigated.

The next section (4) is concerned with both the extension of the Raman technique to measure fibre strain in high volume fraction composites and follow the general mechanical behaviour of such composites. The effect of fibre volume fraction upon the distribution of strain in the fibres and the tensile and compressive strengths of the composites is determined.

In the final section (5) the overall conclusions are summarized and suggestions are made of how the project may be developed and extended.

2. STRUCTURE AND MECHANICAL PROPERTIES OF POLYDIACETYLENE SINGLE CRYSTAL FIBRES

2.1 Background

The increasing use of polymers in structural engineering applications has lead to a need to understand the factors which control their fundamental mechanical properties especially as they are now being exploited as high strength materials. Frank [1] pointed out that a polymer single crystal should have high strength and stiffness because of the covalent bonding along the polymer backbone. For example he showed that polyethylene single crystals should have the same stiffness as steel when deformed parallel to the chain direction. Unfortunately it is not yet possible to obtain large single crystals of polymers such as polyethylene. When it is crystallised from solution microscopic lamellar single crystals are obtained in which the molecules are in chain-folded conformations [2]. On the other hand, melt crystallization produces polycrystalline spherulitic material [2]. Similar behaviour is found for other semicrystalline polymers.

A high degree of molecular orientation can be achieved by the solution-spinning of aromatic polyamides into fibres [3]. Good molecular alignment can be obtained by the mechanical orientation of solid polymers [4,5] and the extensional flow in solution [6]. However, because the fibres produced using such techniques are not single crystals the values of stiffness and strength measured for them are significantly less than the theoretically-predicted ones [7].

Over the past few years developments in the area of solid-state polymerization have lead to the preparation of macroscopic single crystals of certain substituted polydiacetylenes [8]. The diacetylene monomer crystals are prepared by conventional solution crystal-growth techniques and are then polymerized by heat, ultra-violet light or ionizing radiation [9]. The polymer single crystals produced are in the form of lamellae, platelets or fibres depending upon the chemical structure of the monomer and the crystallization conditions [9,10]. The crystals have macroscopic dimensions and single crystal fibres several microns in diameter and up to 8cm long can be produced [10]. Although in the past most of the interest in these materials has been concerned with their optical and electronic properties, the fibres are sufficiently large to allow their mechanical properties to be evaluated [10-12]. This present investigation has been concerned with one particular polydiacetylene, the polymer produced by the polymerization of 1,6-di(N-carbazolyl)-2,4-hexadiyne [13] which will henceforth be referred to as polyDCHD.

In this present study the perfection of the structure of polyDCHD single crystals has been demonstrated using both low- and high-resolution electron microscopy. The mechanical behaviour of the crystals has been correlated with the structure

and this has allowed an experimental confirmation of the predicted mechanical behaviour of polymer crystals.

.2 Experimental

2.2.1 Monomer Synthesis

3-(N-carbazolyl)-1-propyne was prepared by the reaction of bromo-propyne with carbazol in the presence of butyl lithium as described by Kennedy, Chalmers and Bloor [14]. This was then dissolved in dioxane and ethylamine added. Oxygen was then bubbled through the solution while it was stirred vigorously and after several hours it was poured into hydrochloric acid (0.1M). The crude monomer product was obtained after extraction with ether and evaporation of the solvent (final yield 50%). The chemical structure of the monomer

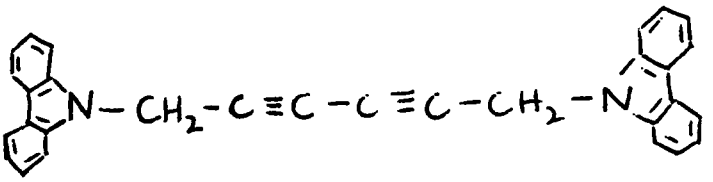

(1,6-di(N-carbazolyl)-2,4-hexadiyne)was confirmed by conventional chemical analysis (Table 1).

2.2.2 Crystal Preparation

It was reported by Yee and Chance [13] that the DCHD monomer forms needle-like colourless crystals when crystallized from common solvents such as acetone, dioxane and toluene. In this present study long, fibre-like crystals were grown from toluene by slow crystallization from solution. A saturated solution of the monomer in toluene was prepared at 80°C and the solution cooled at 5°C per day to 50°C where it was left for a further two days. By this method colourless fibres, which turned pale blue after a few hours exposure to daylight at room temperature, were obtained.

In addition, small crystals suitable for study in a transmission electron microscope were prepared by allowing a dilute (0.001M) solution of the DCHD monomer in xylene to evaporate on a carbon film on standard copper electron microscope grids. This produced a large number of thin (<100nm thick) crystals on a carbon substrate.

The crystals were polymerized using 40 Mrad of γ-rays from a ^{60}Co source and a dose-rate of 1 Mrad/hour. This dose of radiation was found to be sufficient to polymerize the polyDCHD fully such that no residual monomer could be extracted using good solvents.

2.2.3 Electron Microscopy

The crystals were examined using conventional transmission electron microscopy (TEM), high-resolution electron microscopy (HREM) and scanning electron microscopy (SEM). Different specimen preparation techniques were used in each case.

Crystals for examination by TEM and HREM were prepared as described in the previous section. The electron microscope used in both cases was a JEOL 100 CX (side-entry goniometer, C_s = 2.8mm) operated at 100kV. Because polyDCHD suffers radiation damage in the electron microscope [15], a minimum exposure technique was adopted for the investigations and high-speed X-ray film was used. For the conventional TEM a magnification of 5000x was employed and the beam deflected between exposures. This allowed several (~6) bright- and dark-field micrographs and selected area diffraction patterns (SADP's) to be obtained from the same area of crystal before significant damage occurred. Radiation damage was more critical for the HREM studies which involved a magnification of 100,000x. In order to minimise damage, focussing was carried out on an area near to the area of interest. The beam was then deflected while the crystal was translated and finally the micrograph obtained using a relatively short exposure time (3s). Further details of the HREM technique are given elsewhere [15].

Both deformed and undeformed polyDCHD single crystal fibres were examined in an SEM (JEOL 50A). The crystals were made conductive by sputter-coating with a thin layer of gold (~10nm) and earthed using silver paint. They were examined using an accelerating voltage of 15kV and the magnification was calibrated using a fine mesh of known dimensions.

2.2.4 Mechanical Testing

PolyDCHD fibres were mounted across holes between 10mm and 20mm in diameter (depending upon the fibre length) in 0.22mm thick paper tabs. The fibres were bonded to the paper with Durofix adhesive. The tabs were then suspended between spring-loaded fibre-testing jaws attached to an Instron mechanical testing machine. After the fibres in the tabs had been carefully aligned the paper edges were burnt away so that the fibres could be deformed parallel to their length.

The fibres were deformed at different strain-rates of between 0.002 and 0.02 min^{-1} using load cells with a maximum capacity of 0.5kg or 1kg. The extension of each fibre was measured directly by monitoring the movement of marks on the gauge length of the fibre using a travelling microscope. It was estimated that by using this method the strain could be measured to an accuracy of $\pm$ 5% at 1% strain.

The load was recorded automatically on a chart recorder and the stress determined from the load divided by the original cross-sectional area of the fibres. The original crystal

dimensions were determined by examining each fibre after failure in the scanning electron microscope and measuring the dimensions of the undamaged part. The cross-sections of the fibres were found to be approximately rectangular and the dimensions quoted are "effective diameters", i.e. the diameter of a cylindrical fibre with the same cross-sectional area. These measurements gave an accuracy of $\pm$5% in the determination of stress.

Creep tests were also performed at room temperature (22 ± 2^0C) and elevated temperatures using a specially-constructed creep rig. A constant force was applied to single fibres using weights and a pulley system and the fibre extension was again monitored using a travelling microscope. It was estimated that using this technique the stress and strain could both be measured to an accuracyof $\pm$5%. The specimens could also be heated at constant temperatures up to 150^0C and held at $\pm5^0$C whilst the creep behaviour was evaluated.

2.2.5 Differential Scanning Calorimetry

The thermal stability of the polyDCHD fibres was examined by differential scanning calorimetry (DSC) using a Du Pont 900 Thermal Analyser. The technique involves the heating in the same chamber containing an inert atmosphere, a few milligrams of fibres in a sealed aluminium container and a reference sample consisting of an empty container. The heating rate was kept constant at 10K/min and the temperature difference (ΔT) between the sample and reference was monitored continuously.

2.3 Structure

The crystal structure of polyDCHD has been determined using X-ray diffraction [16,17] to a high degree of precision. Details are given in Table 2. In this present study the structure and morphology of the polyDCHD single crystal fibres have been investigated using electron microscopy and this is related to mechanical properties in subsequent sections.

2.3.1 Morphology

It was found that the polyDCHD crystals have a ribbon-like morphology as shown in Figure 1a. Previous investigations have established that the polymer chains are parallel to the fibre axis and that the smooth faces of the crystals can be indexed as crystallographic planes [17]. However careful examination of the crystals has shown that there are also steps on the surface of the crystals (e.g. Figure 1b) which have probably formed during the growth of the monomer crystal. These steps make angles typically of about 20^0C with the fibre axes on the polyDCHD crystals and the step height is normally about 1/10 of the fibre diameter.

The different crystal faces can be seen more clearly in Figure 2 which shows optical micrographs of polished perpendicular sections of polyDCHD fibres which have been embedded in an epoxy resin. The three principal faces (010),

{210} and {2$\bar{1}$0} have been indexed using the crystallographic information in Table 2.

An example of the microscopic crystals used for transmission electron microscopy is given in Figure 3. The crystals shown in this micrograph have their fibre axes parallel to the chain direction and are similar to the crystal shown in Figure 1a but considerably smaller. The crystals also have the three types of faces shown by the crystal in Figure 2 and they generally lie on the carbon film with one of these faces parallel to the plane of the film. Hence a variety of [uv0] SADP's are obtained from different crystals as shown in Figure 4. These correspond to beam directions of [1$\bar{1}$0], [120] and [140] which are all perpendicular to the [001] chain direction and fibre axis. This should be contrasted with another polydiacetylene, the toluene sulphonate derivative, polyTSHD which has a similar crystal structure [18] but for which the crystals have a lamellar rather than fibrous habit. For polyTSHD crystals always lie with their (010) faces parallel to the carbon film and hence the electron beam parallel to the [120] direction [19].

Figure 5 shows a high magnification transmission electron micrograph of the edge of a thin polyDCHD crystal containing a step. It can be seen that the base of the step is extremely sharp with a root radius of about 4nm. This is typical of many similar steps that have been observed in other crystals. In contrast to the macroscopic fibres it was found that the steps made angles of between 20^0 and 60^0 with the fibre edges. The slightly different geometry of the steps in the microscopic crystals was probably due to the different methods of crystal growth employed for the two types of crystals (Section 2.2).

2.3.2 Lattice Imaging

A powerful method of determining the degree of internal perfection in crystals is to directly image the crystal lattice at high magnification using the HREM technique [15]. This is normally very difficult with polymer crystals but it has been found recently that certain polydiacetylene crystals are sufficiently resistant to radiation damage in the electron microscope that lattice images can be obtained [15, 20]. Figure 6 shows a (010) lattice image obtained from a polyDCHD crystal with fringes parallel to the chain direction at a spacing of 1.2 $\pm$ 0.1nm. The regular, parallel nature of the fringes which are parallel to the chain direction shows that the crystals have a high degree of molecular alignment and internal perfection. It was found in an earlier investigation [15] that extremely regular lattice images are obtained and that only very occasionally are defects such as chain-end dislocations encountered.

2.3.3 Thermal Stability

The thermal stability of polyDCHD was determined by DSC and a typical thermogram is shown in Figure 7. The base-line is horizontal to about 300^0C. Above this temperature there is

evidence of a slight exothermic reaction but there is not a large exotherm until the material is above 450°C. This exotherm appears to be due to degradation and there is no evidence of any melting having taken place in the polyDCHD crystals below at least 500°C. Although it is known that polydiacetylene single crystals have good thermal stabilities the behaviour of polyDCHD is particularly impressive [13]. The high-temperature behaviour depends upon the type of side-group (-R) and it appears that the carbazolyl side-group on polyDCHD gives this polydiacetylene extremely good stability.

2.4 Mechanical Propeties

2.4.1 Stress-Strain Behaviour

A stress-strain curve for a single polyDCHD fibre is given in Figure 8. The curve is linear up to a strain of about 1.8% and there is a slight decrease in slope above this strain until fracture occurs at a strain of about 2.8%. Loading and unloading took place along the same paths indicating that there was no detectable hysteresis. The fracture strain of 2.8% is typical of polyDCHD fibres of this diameter (20μm). It tends to increase as the fibre diameter is reduced reflecting the size dependence of the fracture stress and strain [10-12].

This stress-strain curve gives a direct indication of how deformation takes place on a molecular level in polymer crystals. Since the polyDCHD fibres are relatively perfect polymer single crystals the deformation directly involves the stretching and bending of bonds along the polymer backbone. This has been confirmed using Resonance Raman Spectroscopy [21] where it has been shown that the frequencies of the C-C, C=C and C≡C stretching modes in polydiacetylene crystals depend upon the deformation of the crystals, decreasing with applied strain. The consequent reduction in the force constants is one of the factors leading to the slight reduction in slope of the stress-strain curves at high strains.

2.4.2 Young's Modulus

The Young's modulus can be found from the slope of the stress-strain curve in Figure 8. It was found to be 45±2 GPa from measurements upon over 10 different polyDCHD crystals. The modulus of DCHD increases with conversion from monomer to polymer and this behaviour has been followed in detail by Enkelmann and coworkers [17] using Brillouin Spectroscopy. The polymerizing fibres behave like a composite with a monomer matrix reinforced with growing polymer molecules. The modulus increases as the 'volume fraction' of polymer increases with conversion from monomer to polymer.

The general formula of disubstituted polydiacetylene is

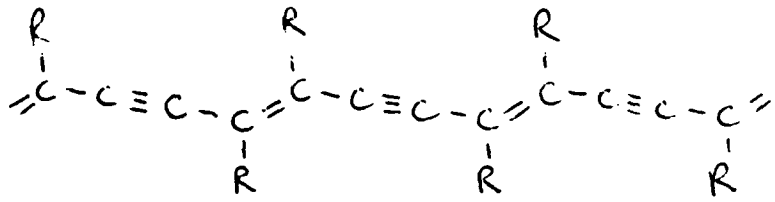

For a particular type of polydiacetylene the value of modulus depends upon the size of the side-group (-R) which controls the effective cross-sectional area of the polymer chain. The carbazolyl side-group on polyDCHD is relatively large and the modulus of 45 GPa reflects this. On the other hand the polyEUHD derivative has a smaller side-group and consequently a modulus of 62 GPa [11]. The dependence of modulus upon side-group size is illustrated in Figure 9 where the modulus E, of polydiacetylene crystals is plotted against the reciprocal of the area supported by each molecular in the crystal, 1/A, (determined from the knowledge of the crystals' structure) for several different derivatives. The proportionality between E and 1/A shows clearly that the modulus is controlled by the chain cross- sectional area. The value of 1/A is also indicated for polyethylene ($A = 0.18nm^2$) which only has hydrogen atoms on the polymer chain. Assuming the two backbones have about the same stiffness then a modulus of 250 - 300 GPa is predicted for polyethylene single crystals - in line with current theoretical predictions [7].

The similarity between the deformation of polydiacetylene molecules and polyethylene molecules is further demonstrated in Figure 10 where a series of force-strain curves are given for the molecules. The force has been determined from the stress and the area supported by each polymer chain in the crystal. Curves are given for both experimental measurements on polydiacetylene single crystals [11, 12] and for different calculated values of modulus for polyethylene [22 -24]. Although the bonding on the two chains is different both have planar zig-zag conformations and it can be seen that the curves have similar slopes. This is further confirmation of the high stiffness of polydiacetylene molecules and shows that the deformation of polydiacetylene fibres takes place by the stretching and bending of the bonds on the polymer backbone.

2.4.3 Fracture Stress

It was found that there was a strong dependence of the fracture stress, σ_f, of the polyDCHD fibres upon the fibre diameter as can be seen in Figure 11. The value of σ_f falls by over a factor of 2 as the fibre diameter is increased from 10μm to 80μm. This type of behaviour has been reported previously for other polydiacetylene single crystal fibres [11, 12] and also for inorganic high-strength fibres [25, 26]. It has been explained in terms of surface defects [27] and will be discussed further in section 5.

2.4.4 Creep

One of the most remarkable aspects of the mechanical properties of polydiacetylene single crystals is that during deformation it has not been possible to measure any time dependent strain or creep. This behaviour is shown in Figure 12 for a polyDCHD single crystal held at constant stress at room temperature. No increase in strain was measured above that produced by the initial loading over a period of up to 80 hours. Preliminary measurements have indicated that creep could not be detected during deformation above ambient temperature up to a temperature of at least 100°C.

Creep and time-dependent deformation are normally a serious draw-back in the used of conventional high-modulus polymer fibres such as polyethylene [28] in engineering applications. Such fibres are normally produced by drawing or spinning and although there is a high degree of molecular alignment, the fibres cannot be classified as single crystals. They contain a high density of defects such as chain-ends, loops, entanglements and some non- crystalline material. This allows the translation of molecules during deformation and consequently leads to creep. In contrast since the polyDCHD fibres are single crystals and the molecules are extremely long there is no mechanism whereby creep can take place even when the temperature is raised above ambient. The equilibrium melting temperature of polydiacetylene single crystals is well above their degradation temperature. This should be contrasted with polyethylene which melts at about 140°C and so has only very limited high-temperature applications.

2.4.5 Compressive Properties

A serious problem with some high-strength polymer fibres, such as Kevlar, is that although they have very good tensile strengths they are rather weak in compression. This is reflected in the strength of composites reinforced with Kevlar fibres being up to 5 times stronger in tension than they are in compression [29, 30]. A simple way of investigating the compressive behaviour of a fibre is to tie it in a knot and see how much damage occurs. If this is done with a Kevlar fibre, the fibre delaminates badly and splits along its length [30]. Figure 14 shows two electron micrographs of a polyDCHD fibre that has been knotted. It can be seen that the fibre tends to deform unevenly, bending sharply in one area (Figure 13a). When the knot is pulled tighter the fibre still remains intact (Figure 13b) but tends to split parallel to the chain direction. It can also be seen that the bending strain is accommodated by the formation of twins which form in the region of the fibre subject to compression. This twinning process has been studied in detail previously [31]. It takes place by the bending of molecules across a well-defined twin boundary and is to a certain extent reversible.

This ability to tie the polyDCHD fibres into tight knots has important implications for their use in composites. The ability to absorb strain by twinning means that they should not break up

as easily as glass fibres during fabrication. It is also likely that composites reinforced with polydiacetylene single crystals will have more comparable tensile and compressive strengths than Kevlar composites as is found in Section 4.

2.5 Theoretical Strength

It is now well-established that the dependence of the strength of strong fibres upon fibre diameter can be explained in terms of surface defects [25 - 27] similar to those seen in Figures 1 and 5. This is because there is a stress concentration at the base of the surface steps or notches which varies with fibre diameter. It is generally accepted [12] that the dependence of σ_f upon the diameter, d, follows a relation of the form

$$\sigma_f \propto 1/d \qquad (1)$$

However, the data from Figure 11 have been replotted in Figure 14, a log-log plot and it can be seen that the dependence of σ_f upon d can be given more closely by the equation

$$\sigma_f \propto 1/d^{0.55} \qquad (2)$$

It will now be shown that this is precisely the behaviour expected for crystals containing surface defects and that from knowledge of the defect geometry the theoretical strength of a defect-free crystal can be determined.

The magnitude of the stress concentration will depend upon the geometry of the surface notch or step. It can be shown that in general the stress concentration factor η at the root of a step or notch is given by

$$\eta = \sigma_0/\sigma_a = k_1 + k_2 a^{1/2} \rho \qquad (3)$$

where σ_a is the applied stress, σ_0 the stress at the root of the defect, a is the notch or step depth, ρ the radius of curvature at the root of the defect and k_1 and k_2 constants which depend upon the geometry of the defect [26, 27].

It has been found that for polyDCHD crystals, similar polydiacetylenes [10, 11] and other high-strength fibres [27] that the depth a scales with the fibre diameter such that

$$a \sim d/m \qquad (4)$$

where m is a constant which is of the order of 10 (cf Figure 1). Putting equation 4 into equation 3, setting $\sigma_a = \sigma_f$ at fracture and rearranging gives

$$\frac{1}{\sigma_f} = \frac{k_1}{\sigma_0} + \frac{k_2}{\sigma_0 (\rho m)^{1/2}} d^{1/2} \qquad (5)$$

where σ_0 now becomes the strength of a defect-free crystal - i.e. the 'theoretical strength'. Hence it is predicted that a plot of $1/\sigma_f$ versus $d^{1/2}$ should give a straight line of slope $k_2 \sigma_0 (\rho m)^{1/2}$ with an intercept of k_1/σ_0. This plot is given in Figure 15 and it can be seen that the data fall on a straight line and give an intercept close to the origin. Considering the approximations involved in the analysis (e.g. equation 4) it appears that the agreement between the data and theory is very good.

In addition, it is possible to determine the theoretical strength, σ_0 if k_2, ρ and m are known or can be found. The value of k_2 depends upon whether the defect is a step or notch and the angle it makes to the fibre surface [26, 27]. For example, for 45^0 steps it has a value of 0.26 and is 0.76 for 90^0 steps [27]. Examination of a large number of steps on macroscopic polyDCHD fibres has shown that they make angles typically of about 20^0 to the fibre surface. Extrapolating the results of the photoelastic stress analysis of Marsh [27] to this angle means that k_2 should be of the order of 0.1 to 0.15. The radius of curvature, ρ, at the base of the step can be determined by examining the edges of thin microscopic crystals at high magnification as seen in Figure 5. Measurements from a large number of crystals have shown that ρ is typically between 3nm and 5nm, hence p has been taken as 4nm. It was shown earlier that m is of the order of 10 and since the slope of the curve in Figure 15 is 0.2 GPa/dμm$^{1/2}$ then the theoretical strength of polyDCHD is calculated to be 3 ± 1 GPa. The rather large uncertainty in the theoretical strength arises from errors in estimating the values of ρ, m and the slope of the curve in Figure 14. Since each molecule supports a cross-sectional area of about 1 nm^2 a strength of 3 GPa corresponds to a force required to break molecules of about 3 nN and a fracture strain of between 6% and 8%. A fracture strain of this size would correspond to a fracture stress of about 20 GPa for polyethylene single crystals. This compares with the highest measured value for highly-oriented polyethylene fibres which is only of the order of 4 GPa [6, 7].

2.6 Summary

It has been shown that the unique structure of polydiacetylene single crystal fibres leads to these materials having high levels of mechanical stiffness and strength. In addition the fibres can possess exceptional thermal stability and have excellent resistance to creep deformation. Polydiacetylene single crystal fibres therefore have great potential as reinforcing fibres in composites and for this purpose offer significant advantages over other polymeric fibres such as high-modulus polyethylene and aromatic polyamide fibres such as Kevlar. The use of polydiacetylene single crystal fibres in composites is pursued in subsequent sections.

3. DISTRIBUTION OF FIBRE STRAIN IN A MODEL SINGLE FIBRE COMPOSITE

3.1 Background

It is well established that the composites produced by incorporating brittle high-modulus fibres in a matrix of epoxy resin or metal can have outstanding mechanical properties. This led to their use initially in the high-technology aerospace industry but now they are finding use in more general engineering applications. Many fibres, such as those of glass, carbon or Kevlar, are produced in continuous form but others are available only as short filaments or whiskers and even continuous fibres are often employed as chopped strands, for example, when they are incorporated into moulding compounds. When discontinuous fibres are used the attainment of good mechanical properties depends critically upon the efficiency of stress transfer between the matrix and fibres.

This problem of stress transfer has received considerable attention over the years and the model system usually considered has been that of a single fibre embedded within a matrix under stress. This system has been analysed from a theoretical viewpoint by several workers [32 - 34] and also experimentally using photoelastic stress analysis [35 - 37]. In his classical study, Cox [32] determined analytically both the tensile stresses in the fibre and the shear stresses at the fibre/matrix interface. The relatively simple equations which resulted have made this a very attractive model for numerous applications. The Cox analysis is, unfortunately, based upon an oversimplified model and includes certain assumptions which are not valid in most composites. For example the model assumes that no tensile stress is transferred from the matrix to the fibre through adhesion at the ends. There have been attempts to find better analytical solutions but the results obtained do not differ greatly from the Cox analysis except at the fibre ends [33]. An approach of potentially greater usefulness is the application of finite element analysis. Using this technique Carrara and McGarry [34] have been able to determine the effect of fibre-end geometry upon the distribution of stresses in the fibre and the matrix.

The leading experimental approach to the problem has been the use of photoelastic analysis to determine the stresses in a birefringent matrix, such as an epoxy resin, containing a single reinforcing fibre. Although this technique gives only the matrix stresses it has been found that the shear stresses near the fibre ends are generally higher than given by the Cox shear-lag model. The results of these experiments are in better agreement with the predictions of more sophisticated analytical solutions [33] and finite element analysis [34]. The photoelastic technique does not, however, allow the variation of tensile stress along the fibre to be determined. This is unfortunate since the strength of composites is often limited by fibre fracture in regions of high

fibre tensile stress.

It was shown in Section 2 that Polydiacetylene (PDA) fibres have promising mechanical properties with values of Young's modulus up to 65 GPa and strengths over 1.5 GPa in the fibre direction [11]; the modulus perpendicular to the fibre axis is also considerably smaller. As the single crystal fibres also show no creep and have good thermal stability they have considerable potential as reinforcing fibres in all-polymer composites. The resonance Raman (RR) spectrum of a PDA crystal usually has only four to six intense lines, one of which has a frequency of about 2100 cm^{-1} and corresponds to a vibrational mode dominated by stretching of the triple bond [38]. When tensile stress is applied to the crystal along the direction of the polymer chain this Raman line has been found to shift to lower frequency at a rate of approximately 20 cm^{-1} for a 1% strain [39]. In the present study we have used RR spectroscopy to directly measure the point-to-point variation in strain along a polydiacetylene single crystal fibre embedded in an epoxy resin matrix which was under an applied tensile stress. In this circumstance the fibres behave as if they have an internal molecular strain gauge [40]. It has been possible to determine both the efficiency of stress transfer in the PDA fibre-epoxy resin system and, more generally, to investigate the fundamental mechanisms of reinforcement in fibre composites.

3.2 Experimental

3.2.1 Fibre Preparation

The substituted diacetylene derivative 1,6-di-(N-carbazolyl)-2,4-hexadiyne (DCHD) was prepared by previously described techniques [13, 41]. Monomer crystals with their axial dimension much longer than their transverse dimension were prepared by slow evaporation from toluene solution. The diameter of the approximately cylindrical crystals could be controlled in the 10 to 100 μm range by adjusting the rate of crystallization; the length varied between 5 and 30 mm. Crystals of uniform diameter and free of obvious surface defects were polymerized by exposure to 35 to 40 Mrad of ^{60}Co γ-radiation. As a result of the topochemical reaction, the polymer chains (poly DCHD) formed parallel to the long axis thus creating single crystal polymer fibres. The fibres had a Young's modulus of 45 $\pm$ 1 GPa in the axial direction as shown in Section 2.4.2.

3.2.2 Specimen Fabrication

Single fibre composite specimens were prepared with Ciba-Geigy XD 927 two-part solvent-free cold-setting epoxy using (by weight) 100 parts of resin to 36 of hardener. It had been previously demonstrated that poly DCHD fibres bond well to an epoxy resin [40]. For these experiments it was also important that the epoxy matrix should be sufficiently transparent and free from fluorescence that RR spectra could be measured for embedded fibres. The PTFE mould was half filled with epoxy and allowed to

partially set before the fibre and the rest of the epoxy were added. This ensured that the fibre was approximately at the centre of the 6 mm thick specimen. The results for specimens prepared in this way were the same as for those prepared by the more difficult technique of introducing the fibre into the already filled mould. After setting at room temperature for 24 hours, thin-film resistance strain gauges of gauge factor 2.1 were attached with the same epoxy to the surface of the specimen at the centre of the fibre. With a DVM it was possible to measure the matrix strain to an absolute accuracy of $\pm$ 0.05%. On two specimens strain gauges were placed at various positions on the surface to confirm that the matrix strain was uniform over the full length of the fibre. The finished specimens were cured at 100°C for 16 more hours and then polished to give smooth transparent surfaces. Holes were drilled at both ends to accommodate the clamps used to apply tensile stress: a typical specimen is shown in Figure 16. After completion of the measurements the specimens were sectioned at several points to determine the fibre diameter. Dummy specimens without fibres were subjected to standard tensile test procedures to determine the mechanical properties of the epoxy resin matrix. The Young's modulus of 2.8 $\pm$ 0.3 GPa was in reasonable agreement with the prediction of the manufacturer.

3.2.3 Mechanical Testing

A small tensile loading device was used to apply stress in the fibre direction. The device was mounted on a micrometer slide so that the full length of the fibre could be traversed through the incident laser beam. The RR spectra were measured with 180° backscattering geometry using a double monochromator and photon counting system [43] with the 676 nm line of a Kr ion laser. The laser beam intensity was approximately 5 mW and the focal spot was about 23 μm in diameter; under these conditions there was no risk of damaging the crystal while good positional sensitivity was retained. The 2085 cm^{-1} Raman line of the poly DCHD single crystal fibres could be measured with an accuracy of $\pm$ 2 cm^{-1}; shifts in the frequency could usually be measured with greater precision. Prior to undertaking the composite experiments the shift of this line with tensile strain had been measured for a DCH fibre which was gripped at the ends but otherwise free-standing [10]. The data shown in Figure 17 were very similar to those found for other PDA single crystal fibres [21, 39, 44]; for poly DCHD fibres the Raman frequency was found to decrease at 19.7 $\pm$ 0.4 cm^{-1}/% for tensile strain. Thus measurement of the RR spectrum of a fibre under tensile stress made it possible to determine the strain within a 25μm diameter region on the fibre to an absolute accuracy of about $\pm$ 0.1%. The RR technique measures the strain at the surface of the pDCH fibre since the effective skin depth for Raman scattering at this wavelength is only about 10 nm [43].

3.3 Results and Discussion

3.3.1 Strain at the Fibre Midpoint

Figure 18 shows the axial strain at the midpoint of poly DCHD fibre I in a composite specimen similar to that in Figure 16 as a function of the strain in the epoxy resin matrix when uniaxial tensile stress was applied to the specimen. The strain in the embedded fibre was determined by the frequency of the Raman line, that of the matrix by the attached resistive strain gauge. Thus the matrix strain referred to in this paper is that in the bulk of the specimen which in general will be different from the local strain of the matrix in the vicinity of the fibre. The 4.5 mm long fibre had a diameter of 21μm. Below 0.5% matrix strain the data follow the Reuss line (R) in Figure 18 which has been predicted by assuming that the stresses in the fibre and matrix are equal [45]. Since the modulus of the fibre is approximately 16 times that of the matrix its strain under these conditions is expected to be considerably less than that of matrix. At matrix strains above 1%, however, additional strain in the matrix is matched by that in the fibre. Thus in Figure 18 the data parallel to the Voigt line (V) which was drawn using the assumption that the strain in the fibre and matrix are under conditions of equal stress in the low strain region. At higher matrix strains the strain at the end of the fibre saturates while that in the central portion continues to increase in proportion to the matrix strain. As shown in Figure 21 the length over which the fibre strain rises from its value at the end to that of the central section is equivalent to half the "critical length" l_c. The fibre length must be greater than l_c if the saturation value of the axial strain is to be reached at the midpoint. This length is closely related to the critical length determined by fibre pull-out tests [46-48]. On the fourth loading, Fibre II was taken to such high stress that debonding of the end of the fibre occurred. This is shown by the essentially zero strain over the first 0.5 mm of the fibre in Figure 22c. This was the only instance in which there was an indication that the bonding between fibre and matrix was anything other than perfect; all other specimens suffered matrix fracture before debonding occurred. A fibre treated with epoxy release agent before it was embedded in the matrix was not subject to any axial strain when the matrix was stressed. This showed that frictional forces were insignificant as compared to those arising from adhesion for this polydiacetylene/epoxy composite.

3.3.3 Mechanism of Stress Transfer

Figures 18 and 19 show that in the low strain region (< 0.5%) the composite follows Reuss type behaviour and the axial strain in the fibre is primarily determined by the stress placed upon the fibre through the matrix attachment at the ends. Thus the stress in the fibre is uniform along its length and approximately equal to the stress in the matrix. The fibre modulus is much greater than that of the matrix so its corresponding strain is much less though also uniform along the length of the fibre. Figures 21 and 22 demonstrate both of these features. For matrix strains over

1%, the high strain region, the relative displacement of the fibre and matrix causes a concentration of shear stresses in the matrix in the vicinity of the fibre ends. These shear stresses in the matrix are converted into tensile stresses in the fibre at the fibre/matrix interface as first pointed out by Cox [32]. In this way "grips" are formed on the end of the fibre and additional tensile stresses in the matrix are transferred through them. Thus in the high strain region the additional strains in fibre and matrix are equal and the shear-lag model of Cox should be in at least qualitative agreement with the results of the present experiment. Since the shear-lag model assumes no stress is transferred through adhesion at the ends of the fibre it can make no predictions about the behaviour of a specimen in the low strain region.

The predictions of the Cox model for the relation between axial fibre strain ϵ_f and matrix strain ϵ_m in the high strain region can be summarised in the single equation

$$\epsilon_f/\epsilon_m = 1 - \frac{\cosh(L/2-x)/l_0}{\cosh\, L/2l_0} \qquad (6)$$

where x is the position along a fibre of length L. The constant l_0 is given by

$$l_0 = r\left[\frac{E_f \ln (R/r)}{2G_m}\right]^{1/2} \qquad (7)$$

where E_f is the tensile modulus of the fibre, G_m the shear modulus of the matrix, r the fibre radius and R the separation between fibres. For $L >> l_0$ equation 6 can be simplified to the following form:

$$\epsilon_f/\epsilon_m = 1 - \exp[-x/l_0] - \exp[-(L-x)/L_0] \qquad (8)$$

It can be seen that for positions well away from the fibre ends $\epsilon_f = \epsilon_m$, while ϵ_f decays exponentially to zero as the fibre ends are approached, reaching the 1/e point at $x = l_0$ or $x = L - l_0$. Thus the constant l_0 should be approximately equal to half the critical length l_c determined in the present experiments. Equation 7 predicts therefore that l_c should be directly proportional to the fibre diameter. The results of measurements of l_c for 17 poly DCHD fibres of differing diameter are shown in Figure 23. The data points almost all fall on the straight line passing through the origin within their uncertainty limits, and so agree very well with that prediction. It is impossible,

however, to compare the slope with that predicted by the Cox model since it assumes that other fibres lie within a few diameters of the central fibre and equation 7 has a logarithmic divergence for the case of a single fibre composite specimen.

The finite element analysis of Carrara and McGarry [34] was carried out on single fibre composite specimens of similar elastic properties to the present specimens although it was assumed that the fibres as well as the matrix possessed elastic isotropy. Figure 8 of that paper, in which the axial stress is plotted as a function of position along the fibre, shares two features in common with Figures 21 and 22 in the present paper, in which axial strain is plotted as a function of position. The axial stress and strain in the fibre are simply related by the Young's modulus of the fibre so the two types of plot are equivalent. Firstly, the finite element analysis shows that the axial stress in the fibre rises from a finite value at the end of the fibre to a fairly constant value over the central portion of the fibre. Secondly, the axial stress at the midpoint of the fibre is lower than that applied to the matrix. Unfortunately the finite element analysis is a numerical procedure without an analytical solution. Thus it is not possible to compare the present results quantitatively with those of Carrara and McGarry. It is clear, however, that this approach contains the basic elements necessary to explain the results of the present experiments.

3.3.4 Residual Matrix Strain

When the stress applied to a specimen was removed the matrix strain as determined by the attached strain gauge initially remained finite. The magnitude of this residual matrix strain increased until a limiting value was reached. The applied stress at which the limit was reached was essentially the same as that required to take the composite specimen into the high strain region where additional matrix and fibre strains were equal. As shown in Figure 20 the critical matrix strain required to reach the high strain region was nearly independent of the aspect ratio of the embedded fibre and hence must largely be determined by the matrix alone. This property of the matrix would thus appear to be an important factor in the formation of the "grips" which mark the transition to the Voigt type behaviour. It was also found that this residual strain relaxed over a period of several days as shown by the results for a single specimen in Figure 24. This suggests that the very high shear stresses that lead to the formation of the "grips" take the matrix into a deformed state from which it is difficult to recover. This slow return to elastic behaviour could be described as viscoelastic.

3.4 Summary

It has been demonstrated that it is possible to measure the axial strain in a PDA single crystal fibre in a transparent epoxy resin matrix. For matrix strains below 0.5% the single fibre model composite demonstrated Reuss type behaviour with the axial

stress approximately equal to the tensile stress in the matrix. Above 1% matrix strain the application of additional tensile stress resulted in Voigt type behaviour with the tensile strain in the fibre matching that in the matrix. In the high strain region the simple model of Cox provides a qualitative description which can explain most of the observed results. An approach such as that supplied by finite element analysis, however, will be required to give a quantitative description over the full range of applied stress.

4. MECHANICAL BEHAVIOUR OF HIGH VOLUME FRACTION COMPOSITES

4.1 Background

In this final experimental section the use of the polyDCHD polydiacetylene (PDA) single crystal fibres has been investigated. Three main aspects have been investigated. Firstly, the possibility of using PDA fibres as a strain gauge suggested in section 3 has been demonstrated for the case of a few PDA fibres in a glass fibre reinforced epoxy resin. Secondly, the effect of increasing the volume fraction of fibres upon the distribution of stress in the fibres has been investigated for a PDA/epoxy composite. Finally, the failure behaviour in both tension and compression has been followed for PDA/epoxy composites containing a high volume fraction of fibres. This is of particular interest since the compressive strengths of epoxy composites reinforced with polymer fibres such as Kevlar have been reported [49] as being rather poor in the past.

4.2 Experimental

4.2.1 Fabrication of glass fibre/PDA/epoxy composites

Low volume fraction composite specimens of epoxy resin containing glass fibres were prepared. A PTFE mould was filled with layers of epoxy and aligned glass-fibres. A number of diacetylene fibres were introduced and distributed uniformly near the surface of the specimen. The specimens were then allowed to set and cure as described in section 3.2.2. Strain gauges (gauge factor 2.1) were attached using the same epoxy to different positions on the surface of the sample. The local volume fraction of glass fibres was determined by cross-sectioning the composites at different places and examining them in an optical microscope.

4.2.2 Fabrication of PDA/epoxy composites

Two types of PDA/epoxy composite samples were prepared, one containing a small bundle of fibres and the other having a high volume fraction of fibres. For the first type, the PTFE mould was half-filled with epoxy and allowed to partially set before a bundle of PDA fibres and the rest of the epoxy were added. Again the same procedure was followed for the setting, curing of the resin and the attachment of strain-gauges.

Composites with high volume fractions of PDA fibres were made by filling the mould with alternating layers of resin and fibres (about 50μm in diameter). The same procedure as before for the setting and curing of the resin and the attachment of strain gauges was employed.

4.2.3 Mechanical testing

The variation of strain in the polyDCHD fibres was measured using resonance Raman spectroscopy as described previously in

section 3.2.3. Since the glass fibres and epoxy matrix were both transparent to the laser light, the strain in individual fibres at various positions in the bundles of fibres could be determined.

The high volume fraction PDA fibre composites were also tested to destruction in both tension and compression. The tensile specimens were made by sticking aluminium tabs onto the compression moulded composite bars with the epoxy resin. Compression specimens were produced by moulding cylindrical pieces of epoxy onto the ends of the bars. The specimens were deformed in either tension or compression in an Instron mechanical testing machine. The failure stress was determined from the maximum load and specimen dimensions.

The surfaces of the specimen fractured in tension were examined in a scanning electron microscope (JEOL 50A) after they had first been coated with gold.

4.3 Results and Discussion

4.3.1 Glass fibre/PDA/epoxy composite

Figure 25 shows the behaviour of the middle of polyDCHD fibres embedded within glass-fibre composites for three different volume fractions (V_f). It is apparent that for very low volume fractions (- 3.8%) the behaviour is the same as that observed before for single-fibre composites (section 3), while for samples of relatively higher volume fraction (Figure 25) the Voigt line is closely followed. This would indicate that the Cox model [32] is applicable for composites of a volume fraction beyond a lower limit of about 8%. However, it was found that in these cases the fibre-strain was uniform along the fibre with only a very small drop near the ends. This cannot be explained by the Cox approach [32].

4.3.2 Bundles of PDA fibres in epoxy resin

Figure 26 shows the fibre-strain as a function of the matrix-strain for five different points on the bundle of fibres with a local volume fraction of - 3%. As can be seen, a single fibre type behaviour is observed throughout the bundle. No significant deviations are observed between the five different point and up to about 1.40% matrix strain beyond which debonding takes place in the middle of the bundle.

4.3.3 Fracture of composites

Table 3 shows the failure stresses of composites deformed in either tension or compression. It can be seen that the tensile fracture stresses are about twice those obtained in compression. It can also be seen that the compressive stress appears to be independent of volume fraction whereas that obtained in tension increases with fibre volume fraction. This should be contrasted with the behaviour of composites reinforced with Kevlar fibres

which have tensile strengths of up to five times larger than those obtained in compression [49].

Figure 27 shows three fractured tensile specimens. It can be seen that fracture occurred in the centre of the gauge-length and that fibre pull-out has also occurred. In contrast it can be seen from Figure 28 that the mechanism of failure in compression is completely different. The specimens buckle in a small region but otherwise remain intact.

The surfaces of a composite fractured in tension are shown in Figure 29. It can be seen that there is considerable pull-out of fibres and that fracture of the individual fibres has also occurred. The faceted nature of the fibres can also be seen in Figure 29b.

4.4 Summary

It has been demonstrated that resonance Raman spectroscopy can be used to measure the strain in individual fibres in composites containing polydiacetylene single crystal fibres. This has been done for both bundles of PDA fibres in an epoxy resin matrix and fibres dispersed in a glass fibre reinforced epoxy resin. It has been found that at low volume fractions the strain in the individual fibres is less than that in the matrix whereas when the volume fraction of fibres exceeds about 8% the strain in the fibres and matrix become similar.

The deformation of epoxy composites reinforced with high volume fractions of PDA fibres has been investigated in both tension and compression. It has been found that the strength of the composites in tension is about twice that measured in compression and tensile strengths of up to 150 MPa have been obtained for composites containing over 50% by volume of PDA fibres. Failure in compression occurs by local buckling of the composite whereas fibre pull-out and fibre fracture takes place during tensile deformation.

5. CONCLUSIONS AND SUGGESTIONS FOR FURTHER WORK

It has been clearly demonstrated that polydiacetylene single crystal fibres have a high degree of stiffness and strength and offer considerable promise as reinforcing fibres in an all-polymer composite. In addition it has been shown that resonance Raman spectroscopy can be used to measure fibre strain with a high degree of precision and accuracy and so allow both the fundamental mechanisms of fibre reinforcement to be investigated and enable the efficiency of stress transfer in the polydiacetylene/epoxy system to be evaluated. It has been demonstrated that the simple theories of fibre reinforcement are only approximations of the actual situation. However, it is clear that in the polydiacetylene/epoxy system the stress transfer is good and the system shows a great deal of promise as an all-polymer composite material.

On the basis of this final report it is suggested that future investigations should be along the following lines:

1) Synthesis of stronger fibres

Fibres with better mechanical properties could be produced if the size of the side group on the polymer chain were reduced further. It is suggested that a programme of synthesis of a larger number of polydiacetylene derivatives with smaller side-groups is performed and the mechanical properties of the polymers produced be investigated.

2) Extension of Raman technique

The resonance Raman method offers a unique method of measuring fibre strain. This could be extended to composites with high volume fractions of fibres. It could be used with transparent polymer matrices other than epoxies and with other types of deformation in addition to simple tension. Further studies could be made of the fundamental aspects of fibre reinforcement. Since the matrix strain can be measured using photoelastic stress analysis it is possible to evaluate the entire state of strain in at least simple composites. Combined with finite element analysis this would offer a powerful combination of experimental and theoretical methods of monitoring the mechanisms of fibre reinforcement.

3) Mechanical behaviour of composites

In this present programme of work there was only time to look at very basic aspects of the deformation of the polydiacetylene/epoxy composites. Other aspects which should be followed include the dependence of the strength and Young's modulus upon fibre size and orientation and the dependence of the modulus upon volume fraction. Also the impact behaviour could be of particular interest.

4) Methods of composite fabrication

In this present project only very simple methods of composite fabrication were employed. Since the polydiacetylenes are a new type of reinforcing fibre, they offer

different methods of composite fabrication.
Since the fibres are relatively tough and can be knotted it is highly likely that they may be resistant to fibre attrition which is a problem with the fabrication of short-strain glass-fibre reinforced composites. Other novel methods of fabrication may emerge based on the unusual method of fibre manufacture. The fabrication of these fibres into composites would need to be thoroughly investigated before they could be used on a commercial scale.

ACKNOWLEDGEMENTS

The authors are indebted to Dr. D.N. Batchelder of the Queen Mary College Physics Department for the use of his laser-Raman facility and his close collaboraton in the project. They are also grateful to Professor D. Bloor of the same department for his support and encouragement and help with the preparation of the polydiacetylene fibres.

Finally they would like to thank Dr. F. Rothwarf of the Europan Research Office for his continued interest and support of the project.

REFERENCES

1. F.C. Frank, Proc. Roy. Soc. (London) A319, (1970), 127.

2. R.J. Young, 'Introduction to Polymers', Chapman and Hall, London 1981.

3. J.R. Schaefgen, T.I. Bair, J.W. Ballou, S.L. Kwolek, P.W. Morgan, M. Panar and J. Zimmerman in 'Ultra-High Modulus Polymers', (Ed. A. Ciferri and I.M. Ward), Applied Science, London, 1979, p.173.

4. G. Capaccio and I.M. Ward, Polym. Eng. Sci. 15, (1975), 219.

5. W.T. Mead, C.R. Desper and R.S. Porter, J. Polym. Sci., Polym. Phys. Edn. 17, (1979), 859.

6. A.J. Pennings and K.E. Meihuizen in 'Ultra-High Modulus Polymers', (Ed. A. Ciferri and I.M. Ward), Applied Science, London, 1979, p.117.

7. A.J. Kinloch and R.J. Young, 'Fracture Behaviour of Polymers', Applied Science, London, 1983.

8. G. Wegner, Pure Appl. Chem., 49, (1977) 433.

9. C. Galiotis, R.J. Young, D.J. Ando and D. Bloor, Makromol. Chem. 184, (1983) 1083.

10. C. Galiotis, 'Polydiacetylene Single Crystal Fibres', Ph.D. Thesis, University of London, 1982.

11. C. Galiotis and R.J. Young, Polymer, 24, (1983), 1023.

12. R.H. Baughman, H. Gleiter and N.J. Sendfeld, J. Polym. Sci., Polym. Phys. Edn. 13, (1975), 1871.

13. K.C. Yee and R.R. Chance, J. Polym. Sci., Polym. Phys. Edn., 16, (1978) A31.

14. R.J. Kennedy, I.F. Chalmers and D. Bloor, Makromol. Chem., Rapid Commun. 1, (1980), 357.

15. R.T. Read and R.J. Young, J. Mater. Sci.

16. P.A. Apgar and K.C. Yee, Acta Cryst. B34, (1978), 957.

17. V. Enkelmann, R.J. Leyrer, G. Schleier and G. Wegner, J. Mater. Sci. 15, (1980), 168.

18. D. Kobelt and E.F. Paulus, Acta Cryst. B30, (1974), 232.

19. R.T. Read and R.J. Young, J. Mater. Sci., 14, (1979), 1968.

20. R.T. Read and R.J. Young, J. Mater. Sci., 16, (1981), 2922.

21. C. Galiotis, R.J. Young and D.N. Batchelder, J. Polym. Sci. 21, (1983) 2483.

22. G.B. Strobl and E. Eckel, J. Polym. Sci., Polym. Phys. Edn., 14, (1976), 443.

23. S. Suhai, J. Polym. Sci., Polym. Phys. Edn., 21, (1983), 1341.

24. B. Crist, M.A. Ratner, A.L. Brower and J.R. Sabin, J. Appl. Phys. 40, (1979), 6047.

25. S.S. Brenner, J. Appl. Phys. 33, (1962), 33.

26. A. Kelly, 'Strong Solids', Clarendon Press, Oxford, 1966.

27. D.M. March in 'Fracture in Solids', (Eds., D.C. Drucker and J.J. Gilman), Interscience, New York, 1963.

28. G. Capaccio, G. Gibson and I.M. Ward in 'Ultra-High Modulus Polymers' (Eds., A. Ciferri and I.M. Ward), Applied Science, London, 1979, p.1.

29. J.H. Greenwood and P.G. Rose, J. Mater. Sci. 9, (1974), 1809.

30. M.G. Dobb, D.J. Johnson and B.P. Saville, Polymer 22, (1979), 960.

31. R.J. Young, R. Dulniak, D.N. Batchelder and D. Bloor, J. Polym. Sci., Polym. Phys. Edn., 17, (1979), 1325.

32. H.L. Cox, Brit. J. Appl. Phys. 3, (1952), 72.

33. G.E. Smith and A.J.M. Spencer, J. Mech. Phys. Solids 18, (1970), 81.

34. A.S. Carrara and F.J. McGarry, J. Comp. Mater. 2, (1968), 222.

35. D.M. Schuster and E. Scala, Trans. Metal. Soc. 230, (1964), 1635.

36. W.R. Tyson and G.W. Davies, Brit. J. Appl. Phys. 16, (1965), 199.

37. I.M. Allison and L.C. Holloway, Brit. J. Appl. Phys. 18, (1967), 979.

38. W.F. Lewis and D.N. Batchelder, Chem. Phys. Lett. 60, (1979), 232.

39. D.N. Batchelder and D. Bloor, J. Polym. Sci., Polym. Phys. Edn. 17, (1979), 569.

40. C. Galiotis, R.J. Young and D.N. Batchelder, J. Mater. Sci. Lett. 2, (1983), 236.

41. V. Enkelmann, G. Scheier, G. Wegner, H. Eichele and M. Schwoerer, Chem. Phys. Lett. 52, (1977), 314.

42. C. Galiotis, R.T. Read, P.H.J. Yeung, R.J. Young, I.F. Chalmers and D. Bloor, J. Polym. Sci., Polym. Phys. Edn., to be published.

43. D.N. Batchelder and D. Bloor, in "Advances in Infrared and Raman Spectroscopy", Vol. 11, edited by R.J.H. Clark and R.E. Hester (Wiley Heydon, Chichester, 1983), p.133.

44. V.J. Mitra, W.M. Risen Jr. and R.H. Baughman, J. Chem.Phys. 66, (1977), 2731.

45. R.P. Kambour and R.E. Robertson, "Polymer Science", edited by A.D. Jenkins (North-Holland, London, 1972) p. 687.

46. C.C. Chamis, in "Composite Materials", Vol. 6, edited by E.P. Plueddeman (Academic Press, New York, 1974), p.31.

47. P. Bartos, J. Mater. Sci. 15, (1980), 3122.

48. N.H. Ladizesky and I.M. Ward, J. Mater. Sci. 18, (1983), 533.

TABLE 1

Analysis of the composition of the DCHD monomer

Wt%	C	H	N
Calculated	88.21	4.94	6.86
Measured	87.82	4.79	6.75

TABLE 2

Unit cell parameters and space group of polyDCHD indexed with the chain direction as c

Investigators	Space Group	a/nm	b/nm	c/nm	γ
Apgar and Yee [16] 108.3^0	$P2_1/a$	1.740	1.287	0.491	108.3^0

TABLE 3

Mechanical properties of PDA/epoxy composites

Fibre volume fraction (%)	Compressive failure stress (MPa)	Tensile failure stress (MPa)
25	55	-
30	54	-
36	48	-
48	58	-
27	-	86
36	-	89
55	-	150
57	-	100

FIGURE CAPTIONS

Figure 1 Scanning electron micrographs of a polyDCHD fibre.

a) Low magnification showing surface steps.

b) Higher magnification showing the bases of the steps.

Figure 2 Optical micrographs of polished perpendicular sections of fibres.

a) Approximately hexagonal cross-section fibre.

b) Ribbon-like fibre.

Figure 3 Transmission electron micrograph of polyDCHD crystals showing variety of fibre dimensions.

Figure 4 Selected-area diffraction patterns obtained from polyDCHD crystals in different orientations.

a) Beam direction $[1\bar{1}0]$.

b) Beam direction [120].

c) Beam direction [140].

Figure 5 Transmission electron micrograph of the base of a step on a polyDCHD crystal.

Figure 6 (010) lattice image from a thin polyDCHD crystal showing a spacing of approximately 1.2 nm.

Figure 7 DSC thermogram for polyDCHD crystals (Heating rate 10^0C/min).

Figure 8 Stress-strain curve for a polyDCHD single crystal fibre. The closed circles are for loading and the open ones for unloading.

Figure 9 Dependence of the Young's modulus of polydiacetylene single crystal fibres upon the reciprocal of the area supported by each polymer chain. The line S and the open circles are for values calculated using force-constants determined by Raman Spectroscopy. The line M and the closed circles are for the mechanically-measured ones [11]. The arrow corresponds to the value of 1/A for polyethylene.

Figure 10 Force-strain curves for different polymer molecules. The polyethylene values are calculated ones: 1-[24], 2-[23], 3-[22]. The values for different polydiacetylene derivatives have been measured mechanically; polyEUHD-[11], polyPUHD-[12], polyDCHD - this present study.

Figure 11 Dependence of the fracture stress upon effective fibre diameter for polyDCHD fibres.

Figure 12 Variation of fibre strain with time for a polyDCHD fibre held at a constant stress corresponding to 50% of its fracture strain (given by dashed line).

Figure 13 Scanning electron micrographs of a knotted polyDCHD fibre.

a) Large knot.

b) Tighter knot in the same fibre.

Figure 14 Log-log plot of fibre strength as a function of effective fibre diameter for the data from Fig. 11. The line is a least squares fit to the points (correlation coefficient = 0.96).

Figure 15 Variation of the reciprocal of the fibre strength with square root of the fibre diameter for polyDCHD fibres.

Figure 16 Single fibre composite specimen. The polyDCHD fibre is located at the centre of the specimen while the resistive strain gauge is attached to the outer surface.

Figure 17 Strain dependence of the 1085 cm^{-1} Raman line of a free-standing polyDCHD fibre.

Figure 18 Axial strain at the midpoint of fibre I as a function of matrix strain.

Figure 19 Axial strain at the midpoint of fibre II as a function of matrix strain.

Figure 20 Critical matrix strain for 15 different single fibre composite specimens plotted as a function of the inverse of the aspect ratio of the fibres.

Figure 21 Axial strain of fibre I as a function of the position along the fibre.

Figure 22 Axial strain of fibre II as a function of the position along the fibre: (a) first loading, (b) second and third loadings and (c) fourth loading.

Figure 23 Critical length l, determined for 17 different polyDCHD fibres in the same way as illustrated for fibre I in Figure 5 plotted as a function of the fibre diameter.

Figure 24 Residual matrix strain for a typical specimen as a function of the time elapsed after the removal of the tensile stress.

Figure 25 Axial strains at the mid-points of polyDCHD fibres in glass-fibre/epoxy composites of the different fibre volume fractions (V_f) indicated. The matrix strain is given by e_m.

Figure 26 Axial strains at the mid-points of polyDCHD fibres in a PDA/epoxy composite as a function of matrix strain. The different positions of the fibres in the composite are indicated in the sketch.

Figure 27 Three fractured PDA/epoxy composites showing the mechanism of failure in tension.

Figure 28 Two failed PDA/epoxy compression specimens showing failure by buckling.

Figure 29 Scanning electron micrographs of a polyDCHD reinforced epoxy resin composite.

a) Low magnification micrograph.

b) Higher magnification micrograph showing fibre fracture and pull-out.

(a)

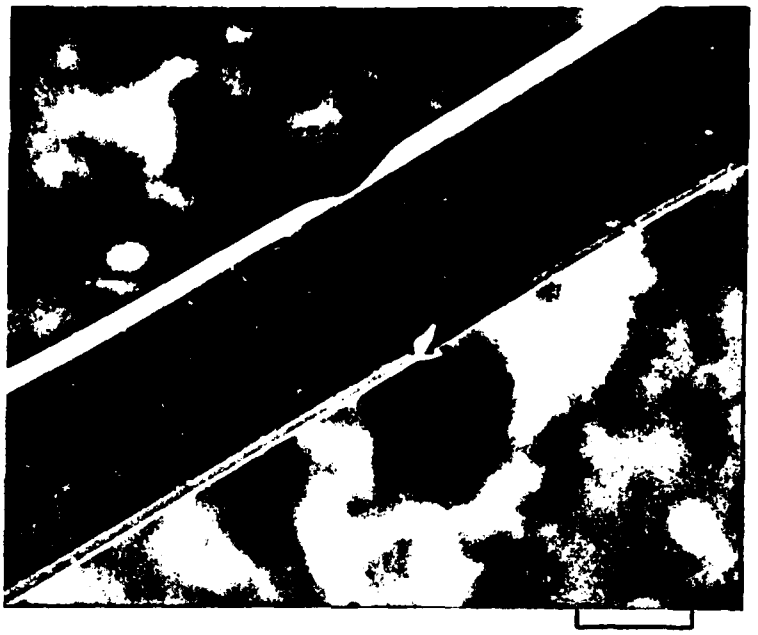

10μm

(b)

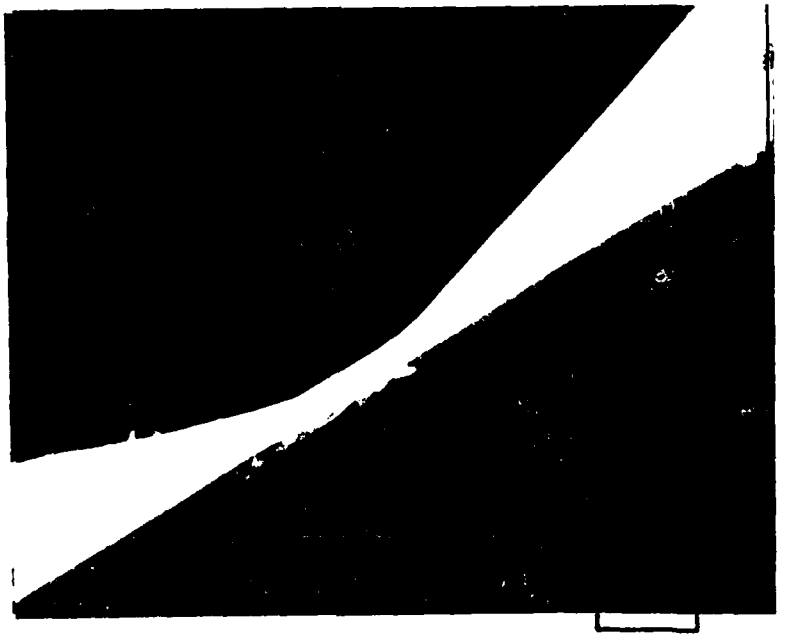

1μm

FIGURE 1

(a)

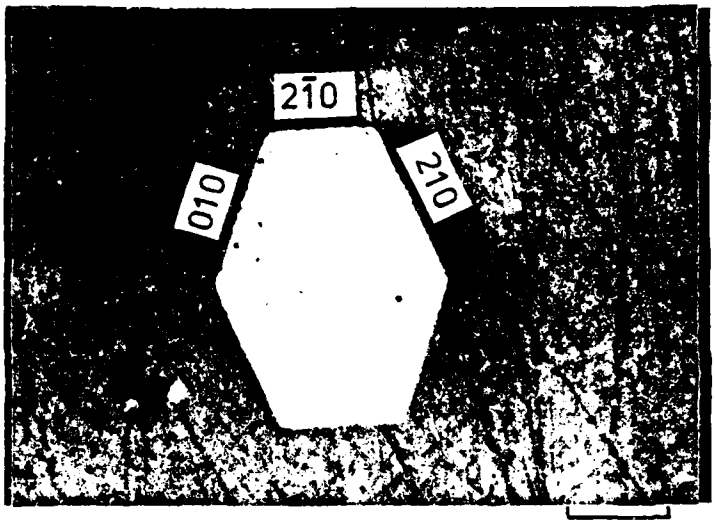

(b)

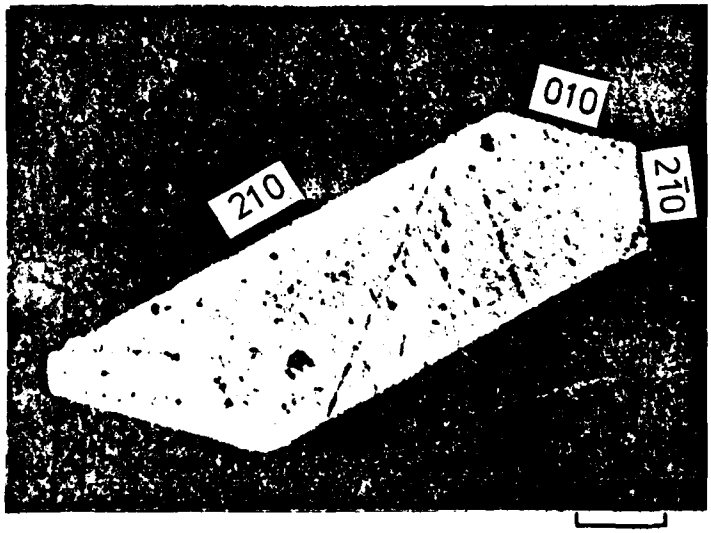

FIGURE 2

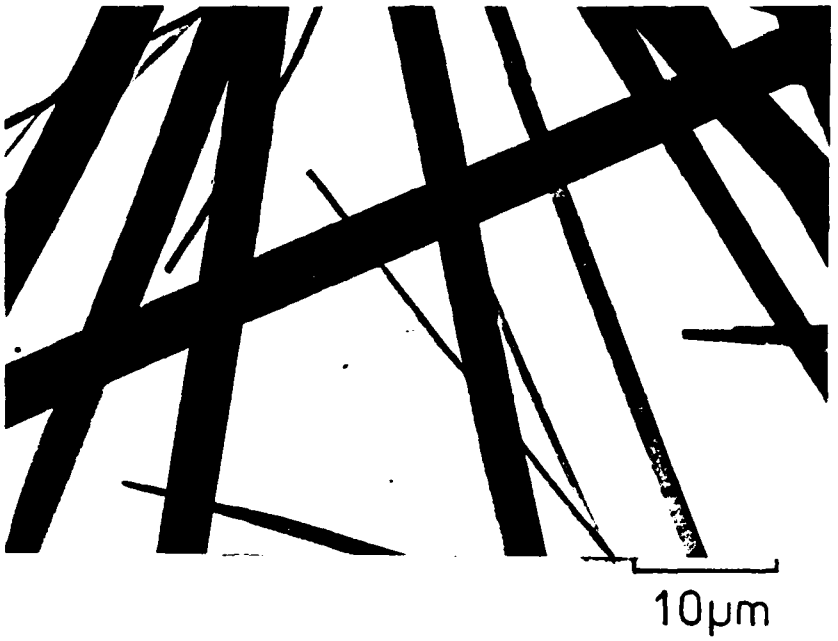

FIGURE 3

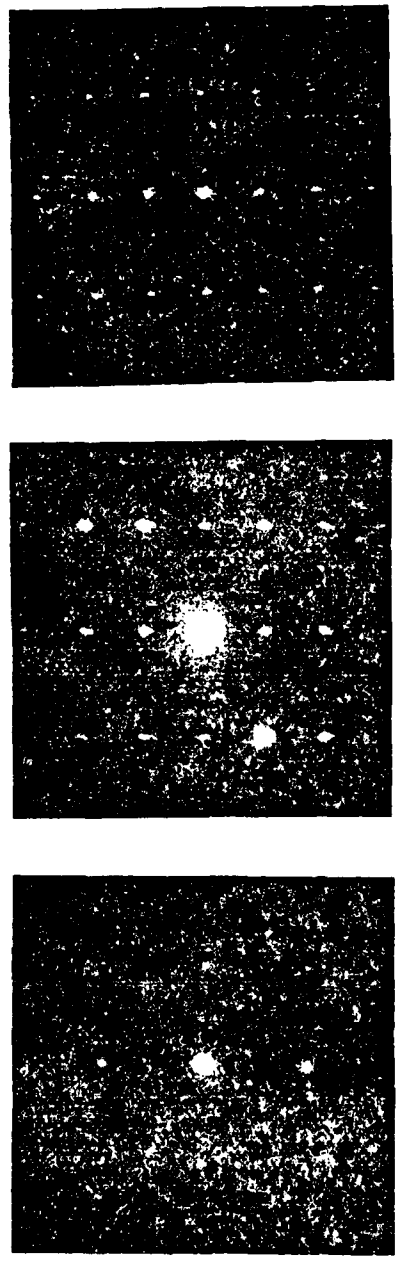

FIGURE 4

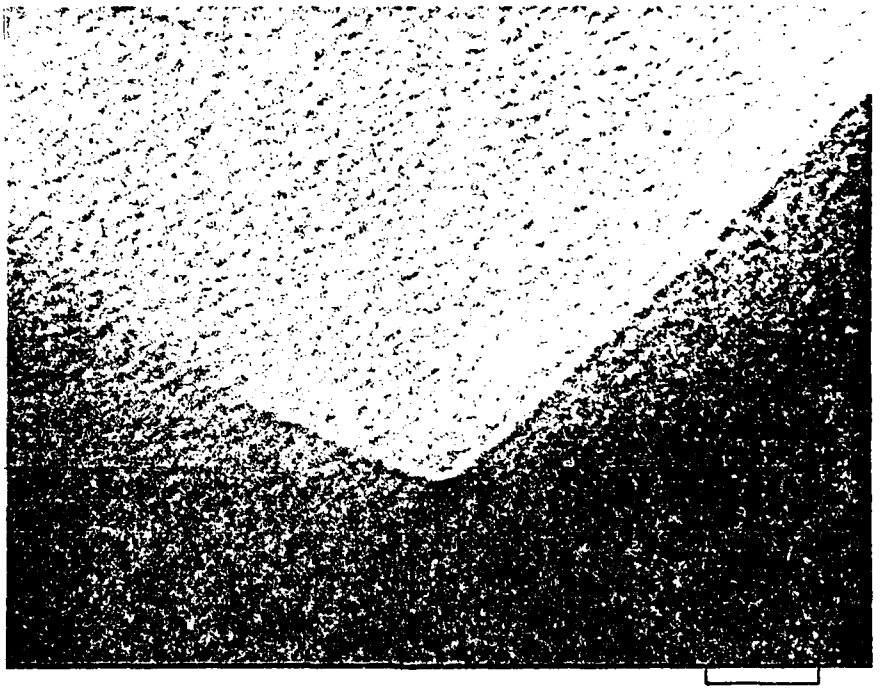

FIGURE 5

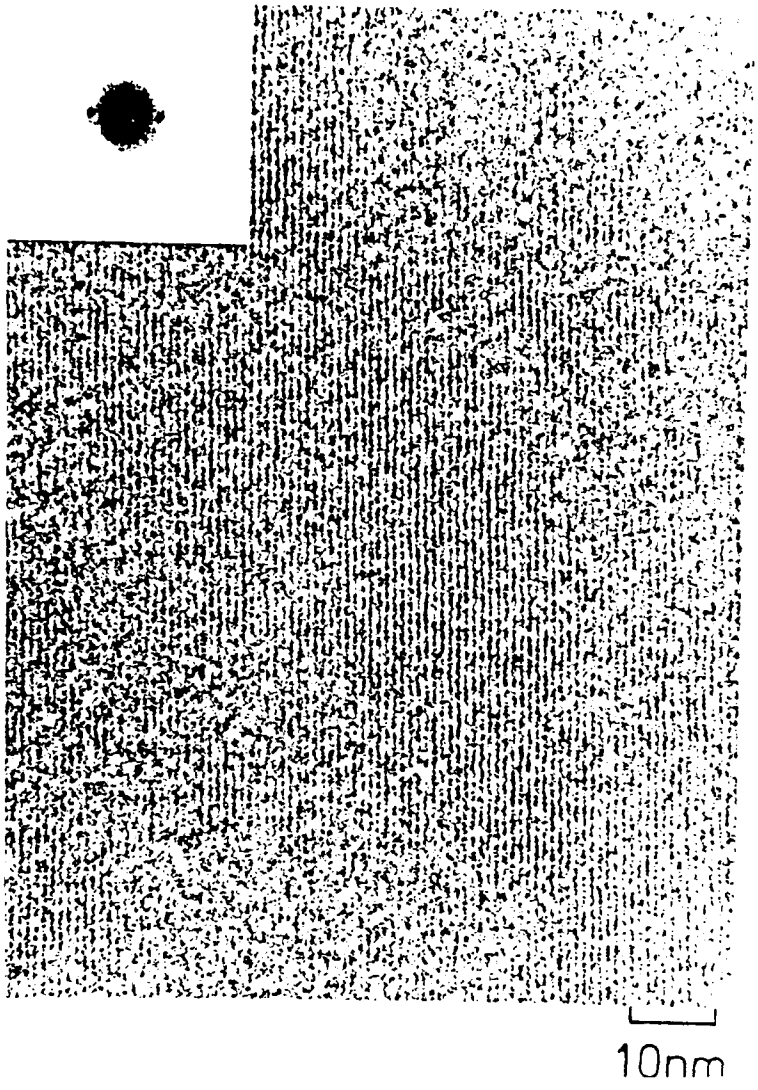

FIGURE 6

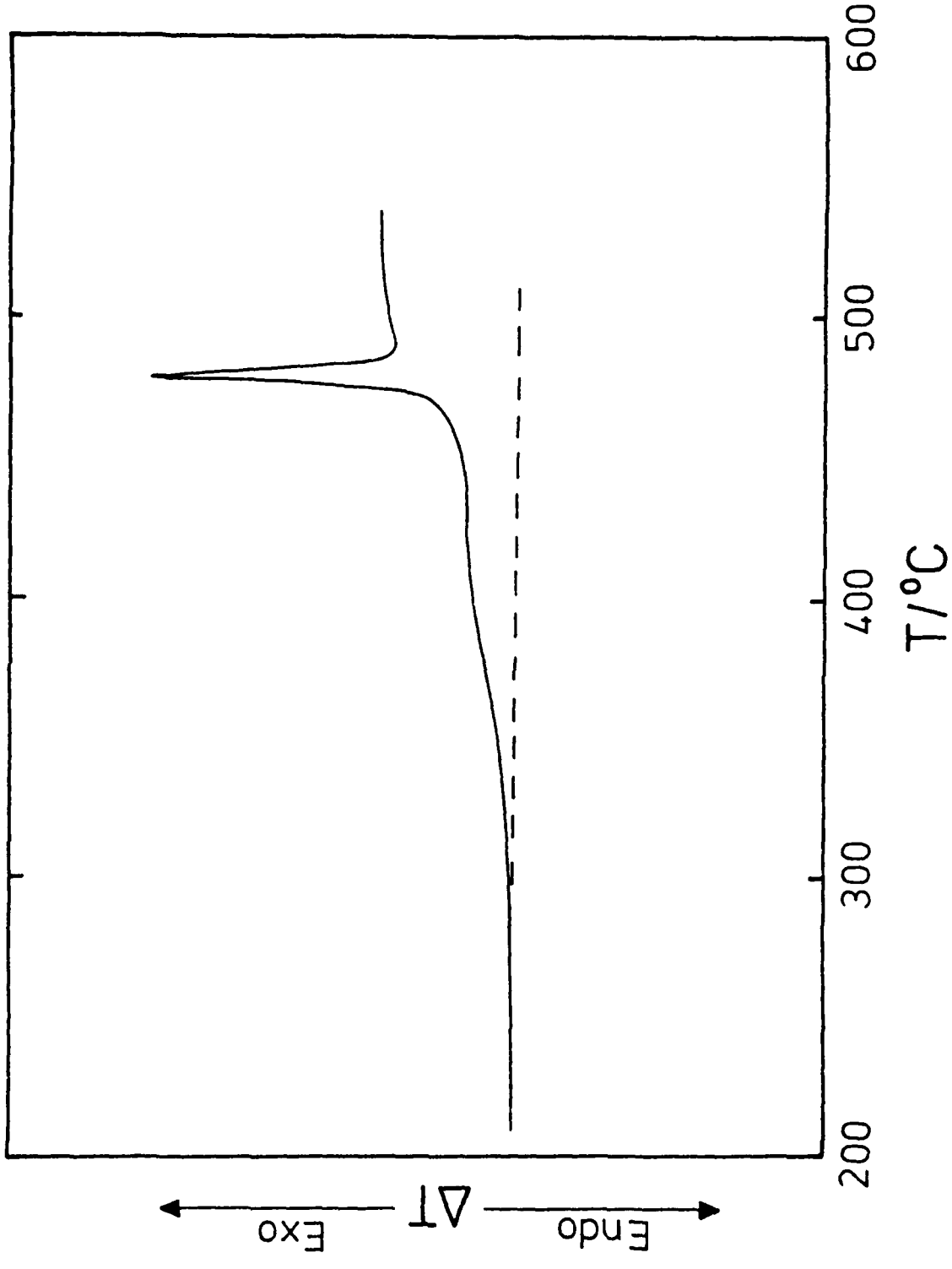

FIGURE 7

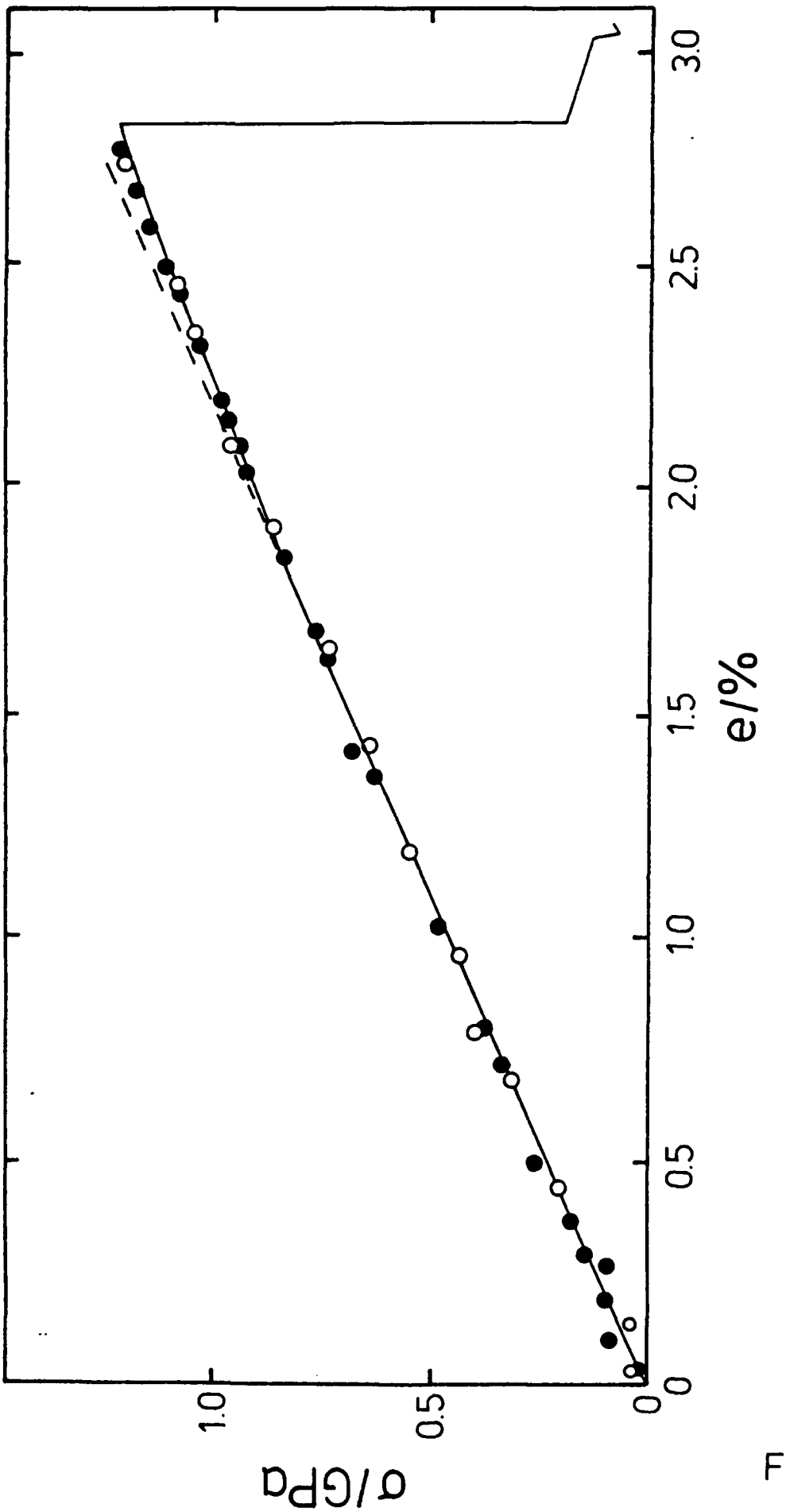

FIGURE 8

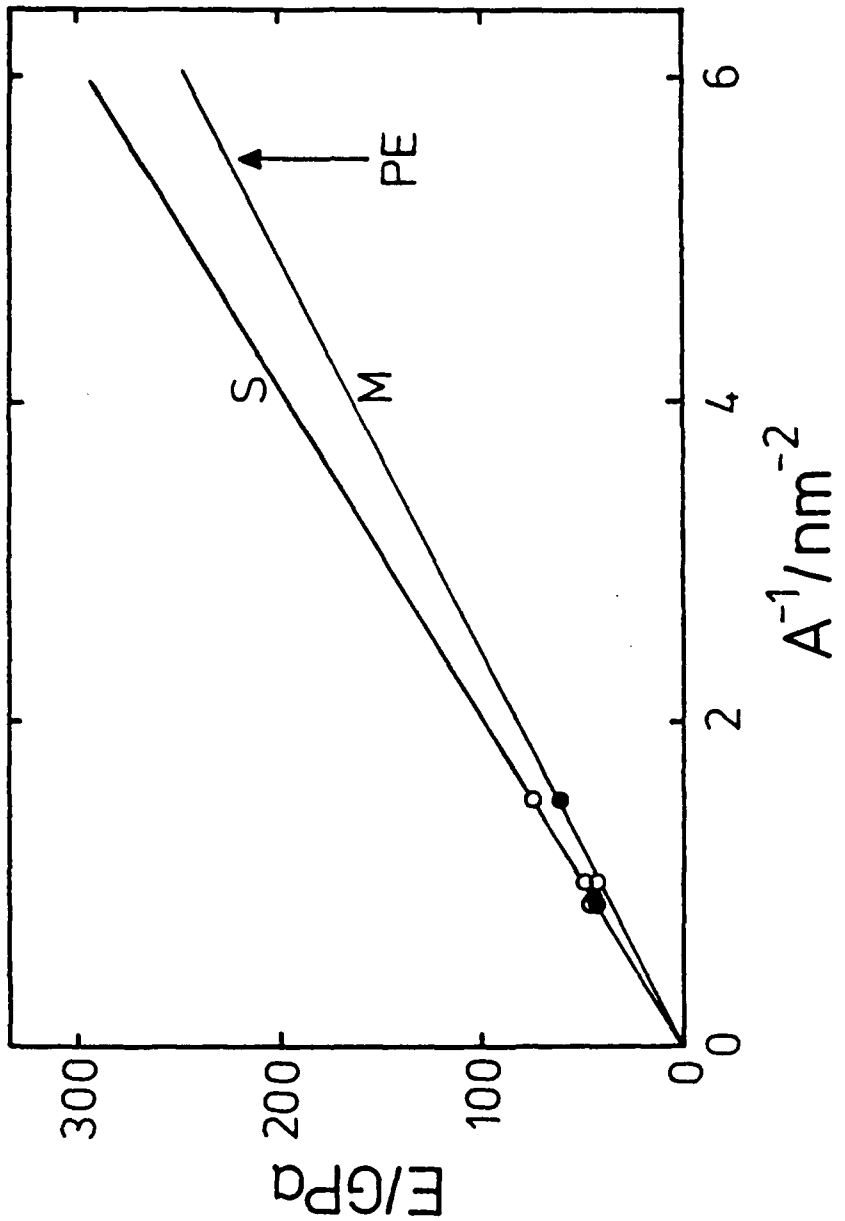

FIGURE 9

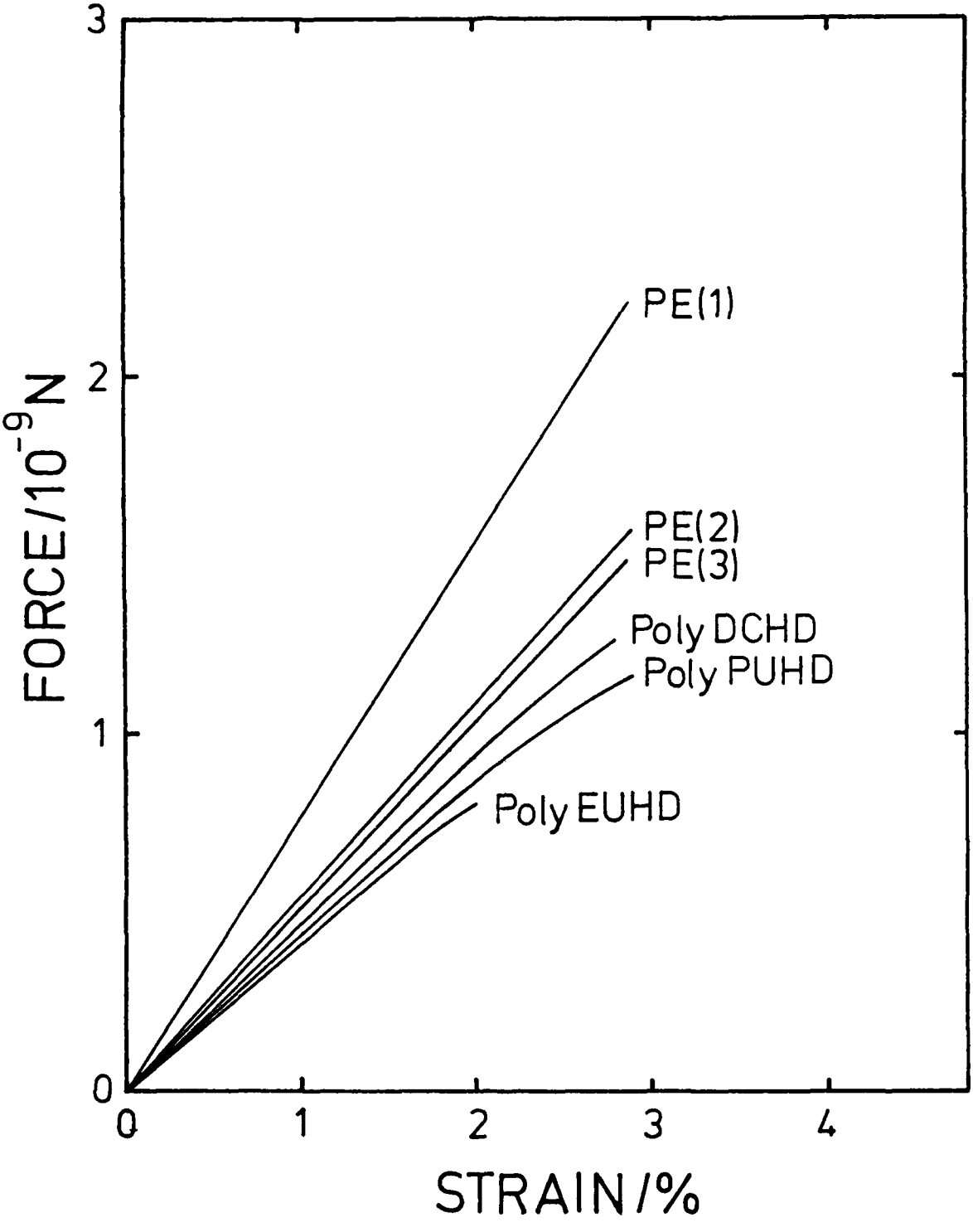
3
2
1
0
0
1
2
3
4
FORCE/10^{-9}N
STRAIN/%
PE(1)
PE(2)
PE(3)
Poly DCHD
Poly PUHD
Poly EUHD

FIGURE 10

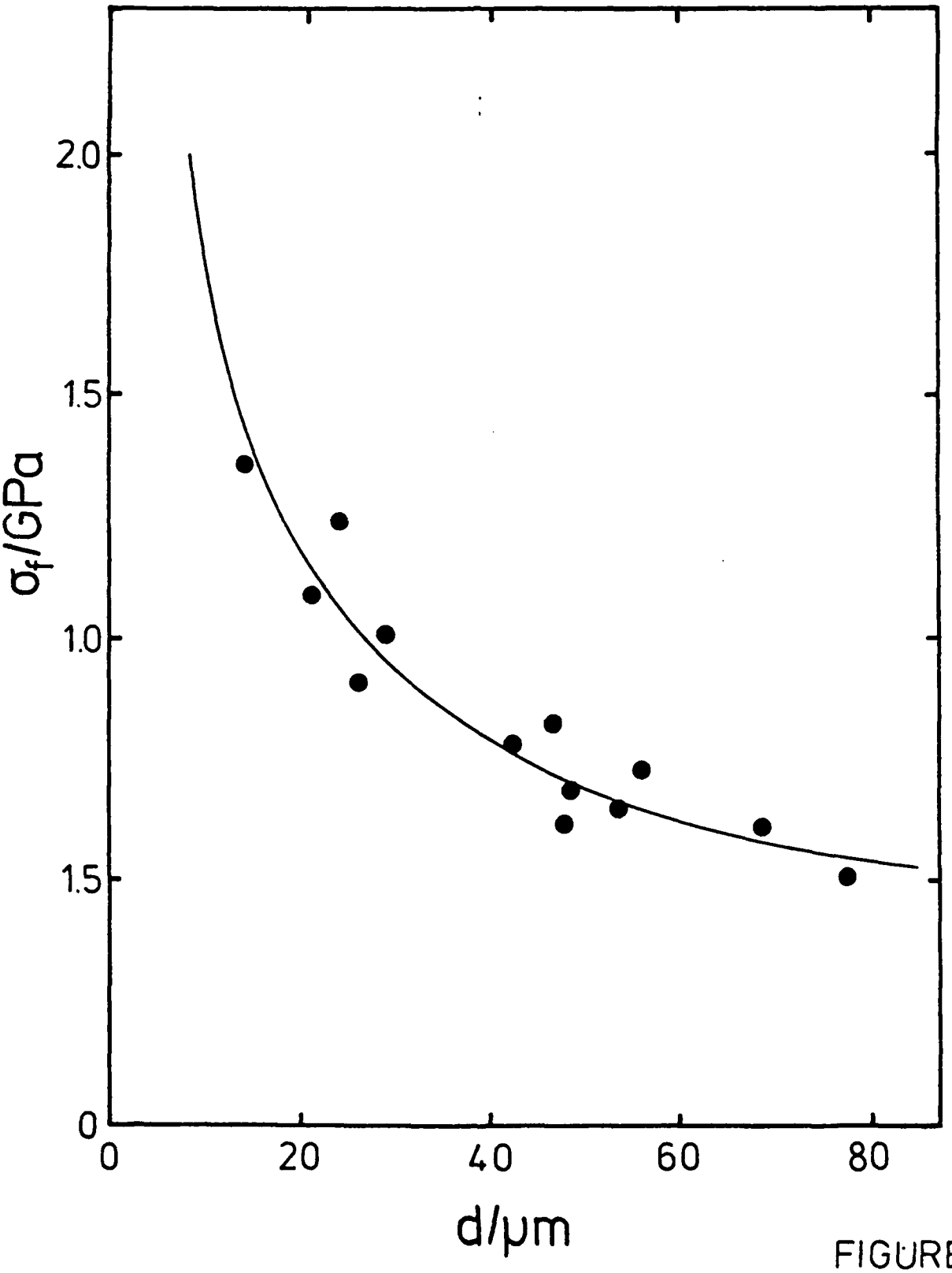

FIGURE 11

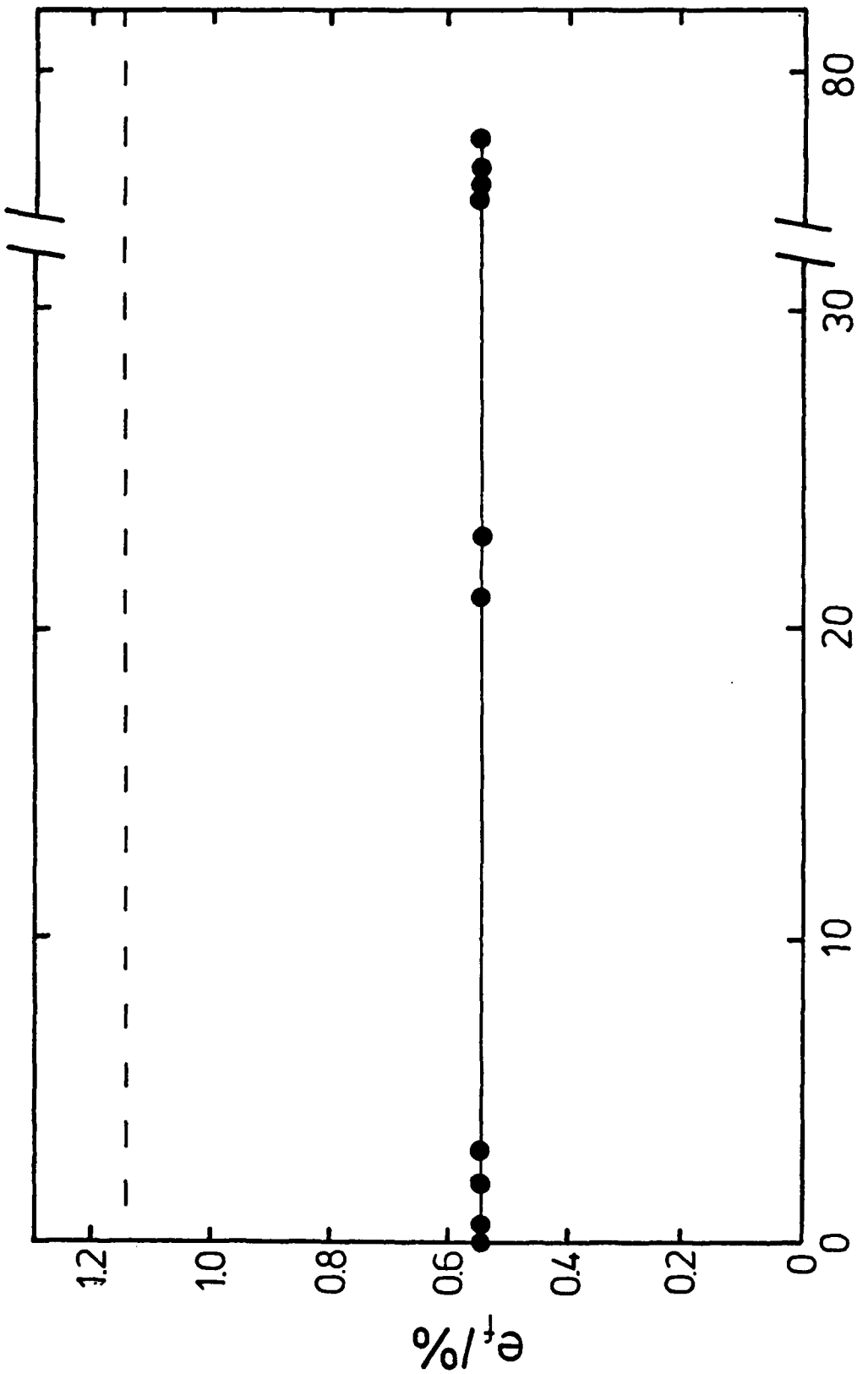

FIGURE 12

(a)

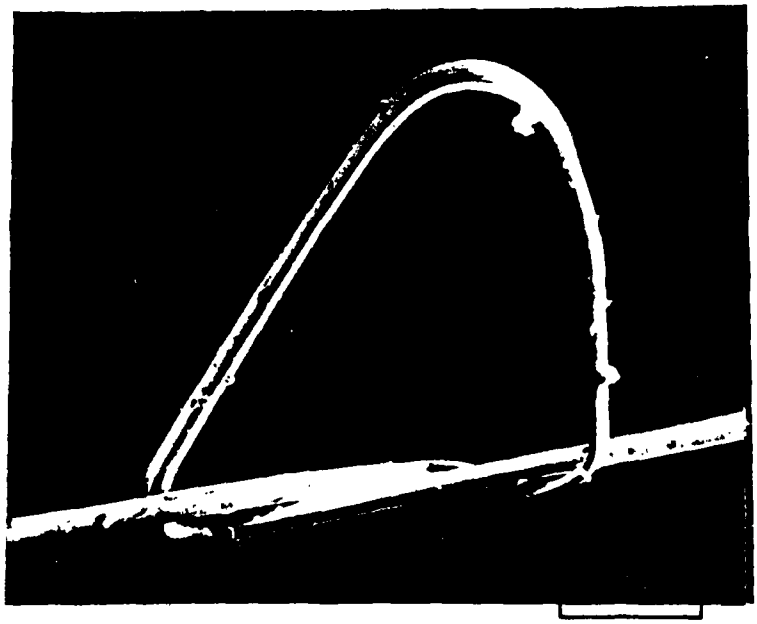

200μm

(b)

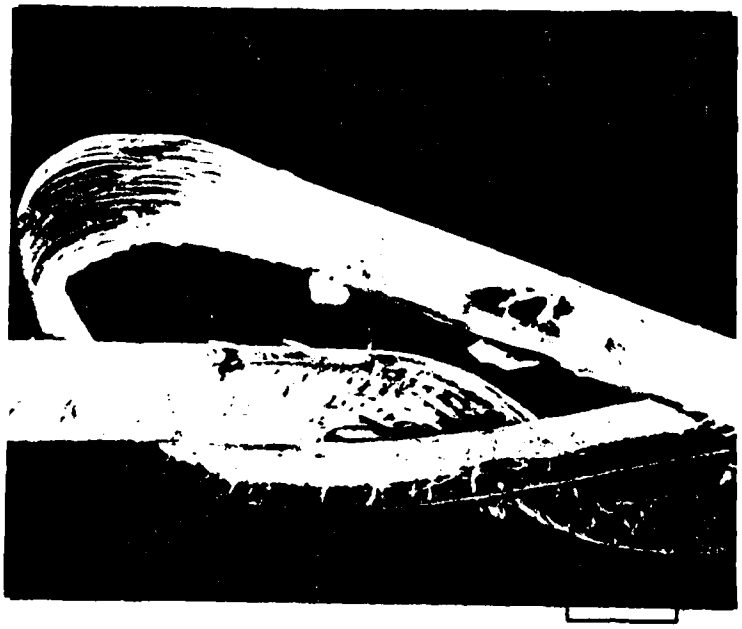

50μm

FIGURE 13

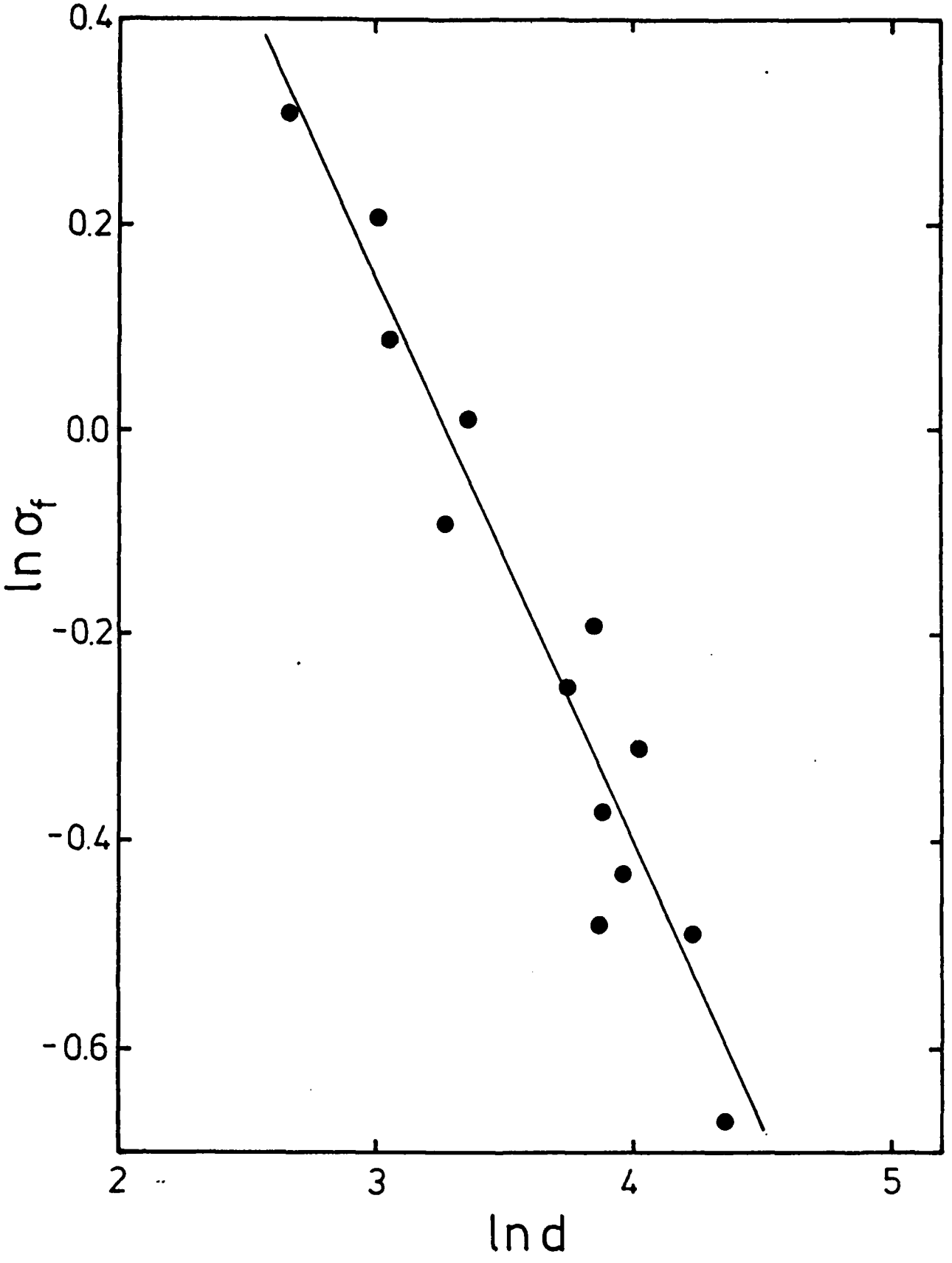

FIGURE 14

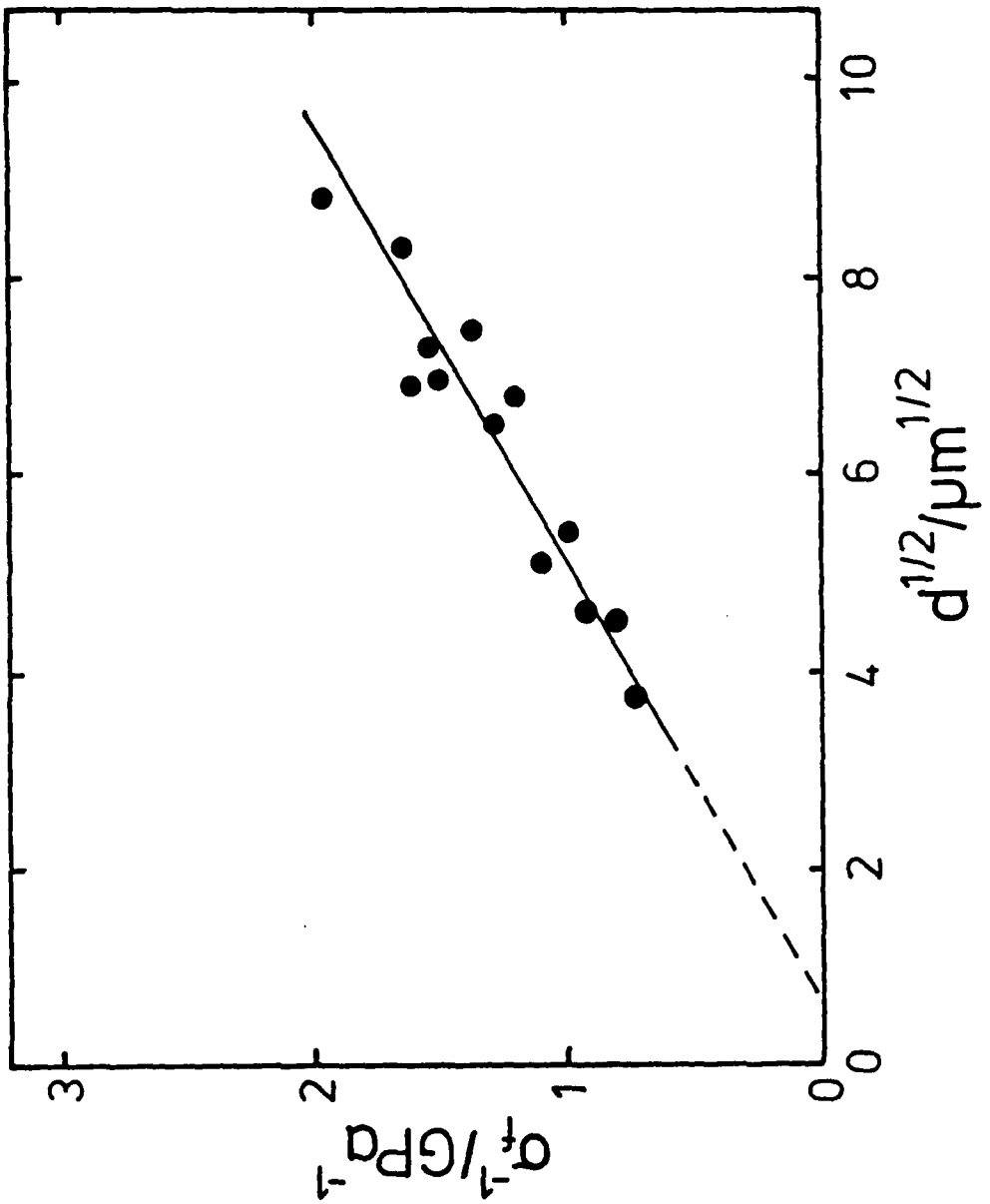

FIGURE 15

FIGURE 16

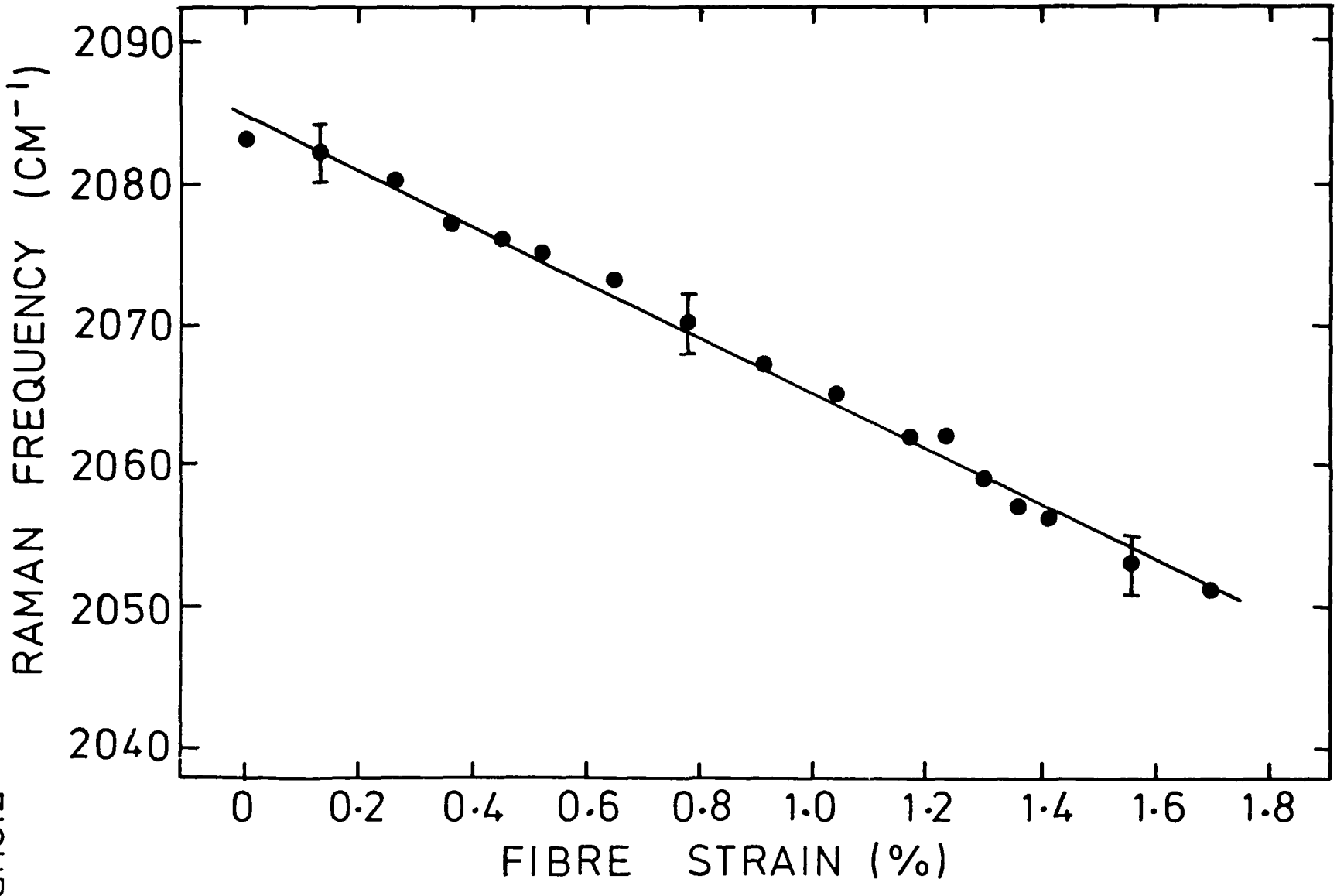
RAMAN FREQUENCY (CM⁻¹)
2090
2080
2070
2060
2050
2040
0
0·2
0·4
0·6
0·8
1·0
1·2
1·4
1·6
1·8
FIBRE STRAIN (%)

FIGURE 17

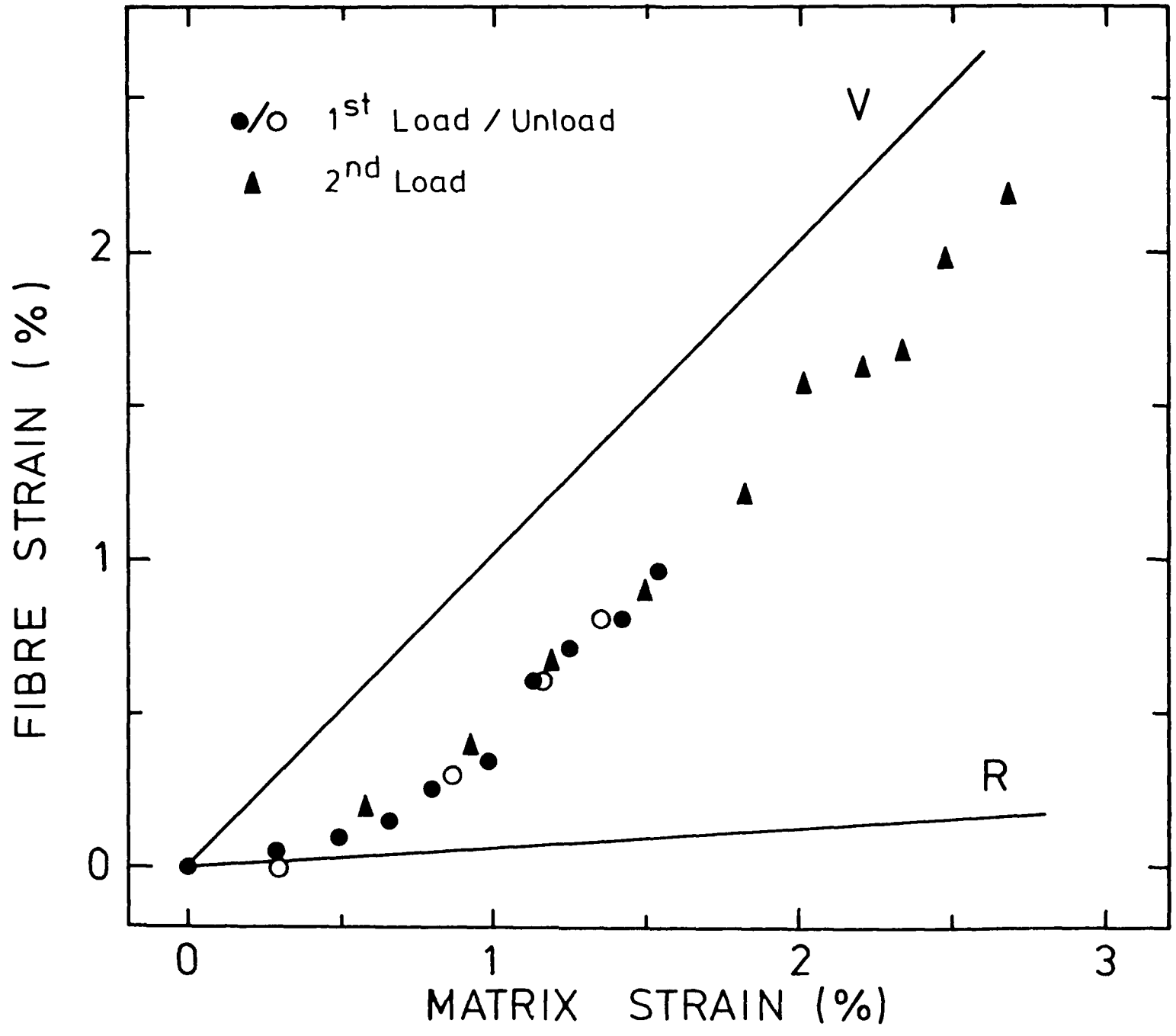

FIGURE 18

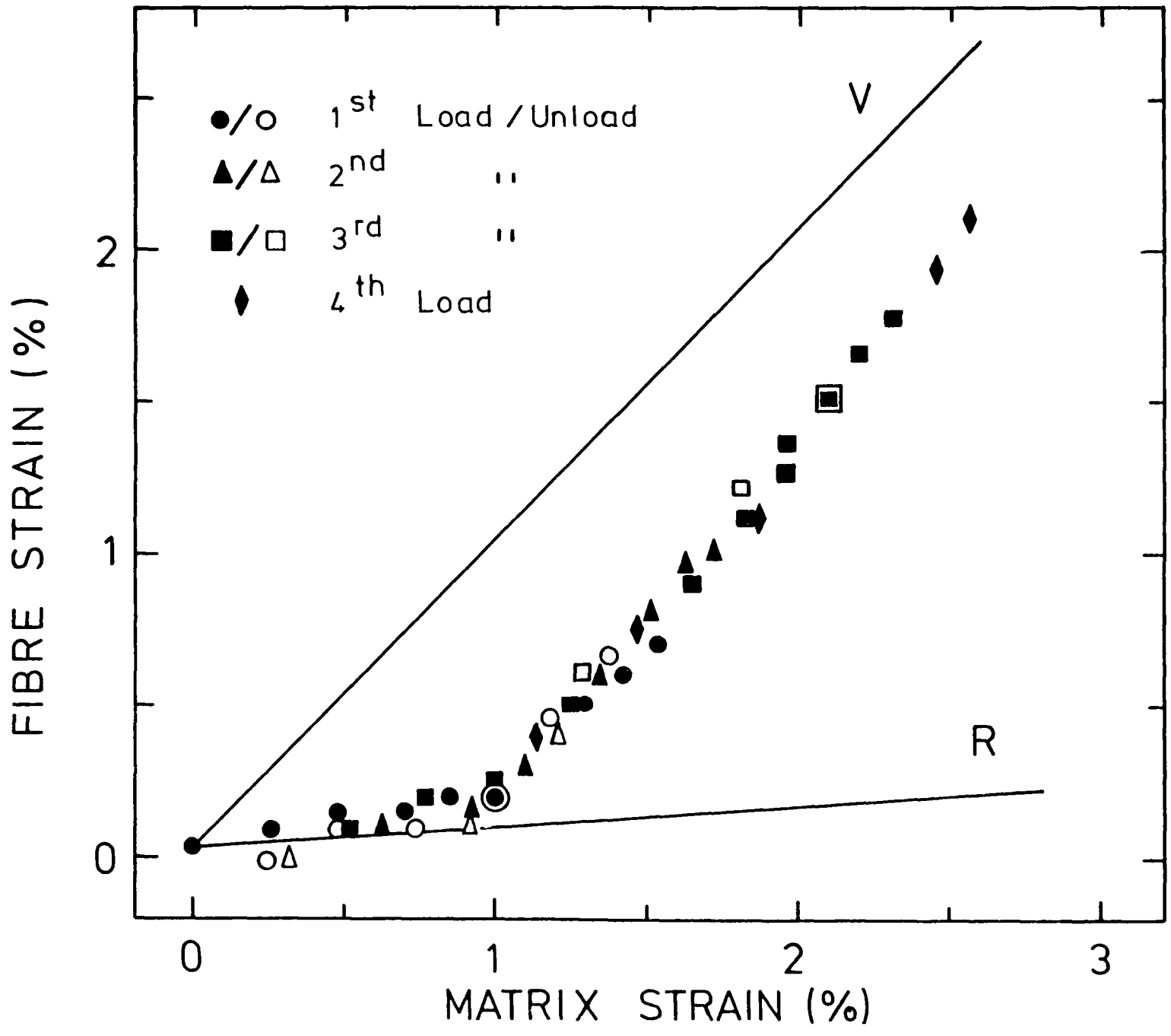
●/○ 1st Load / Unload
▲/△ 2nd "
■/□ 3rd "
♦ 4th Load
V
R
FIBRE STRAIN (%)
MATRIX STRAIN (%)
0
1
2
3

FIGURE 19

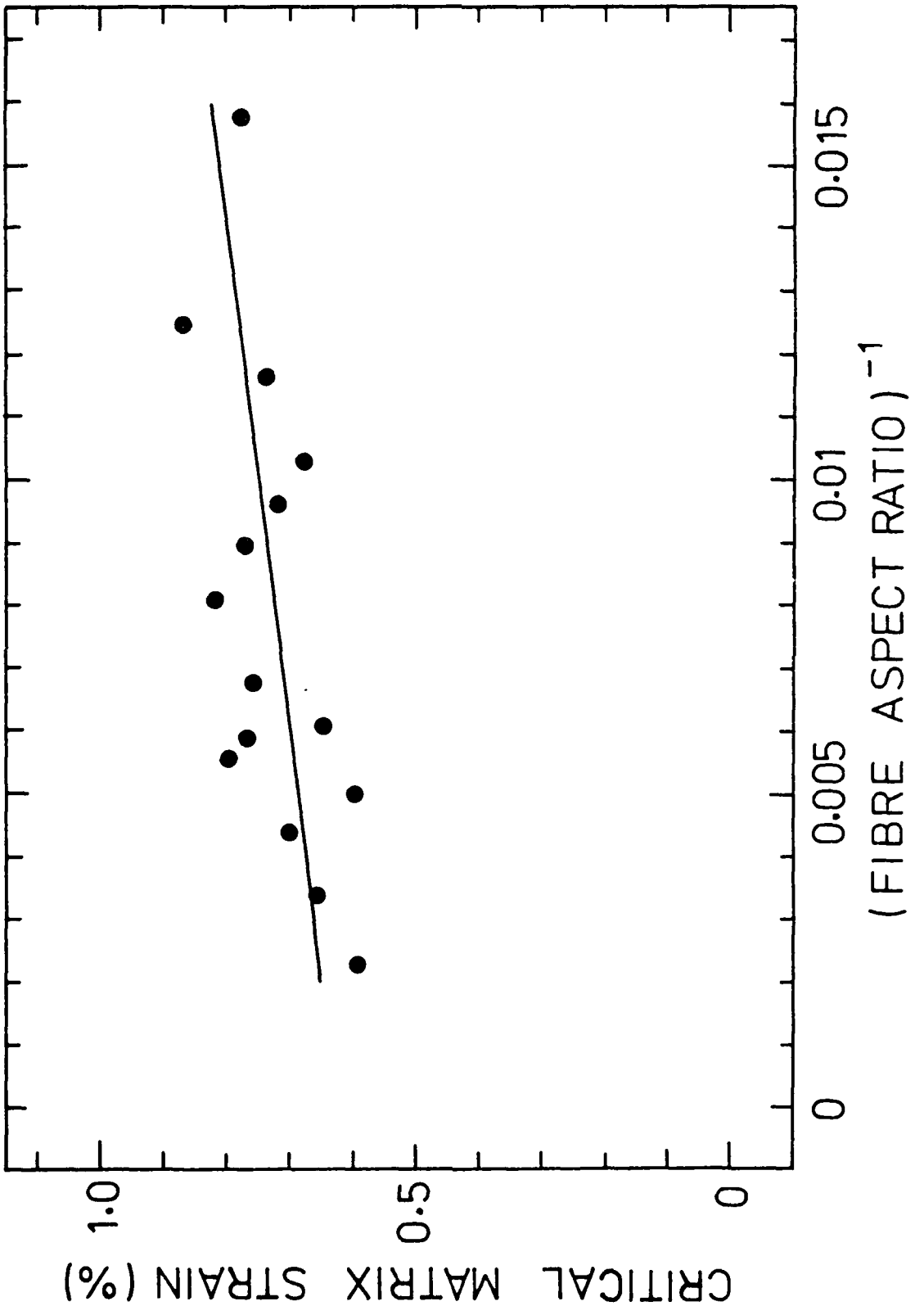
CRITICAL MATRIX STRAIN (%)
1.0
0.5
0
0
0.005
0.01
0.015
(FIBRE ASPECT RATIO)$^{-1}$

FIGURE 20

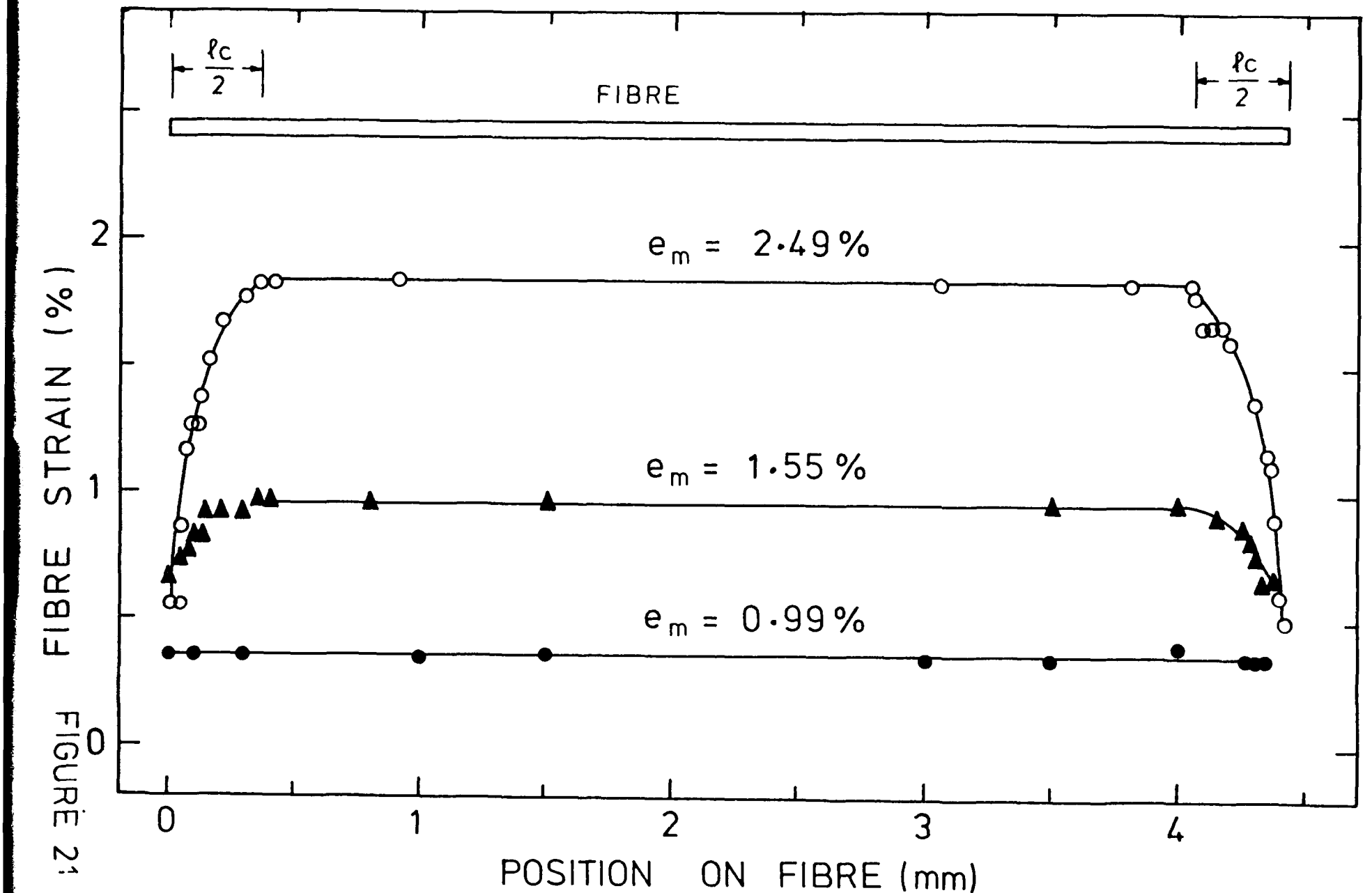
$\frac{\ell_c}{2}$
FIBRE
$\frac{\ell_c}{2}$
e_m = 2·49 %
e_m = 1·55 %
e_m = 0·99 %
FIBRE STRAIN (%)
0
1
2
0
1
2
3
4
POSITION ON FIBRE (mm)

FIGURE 21

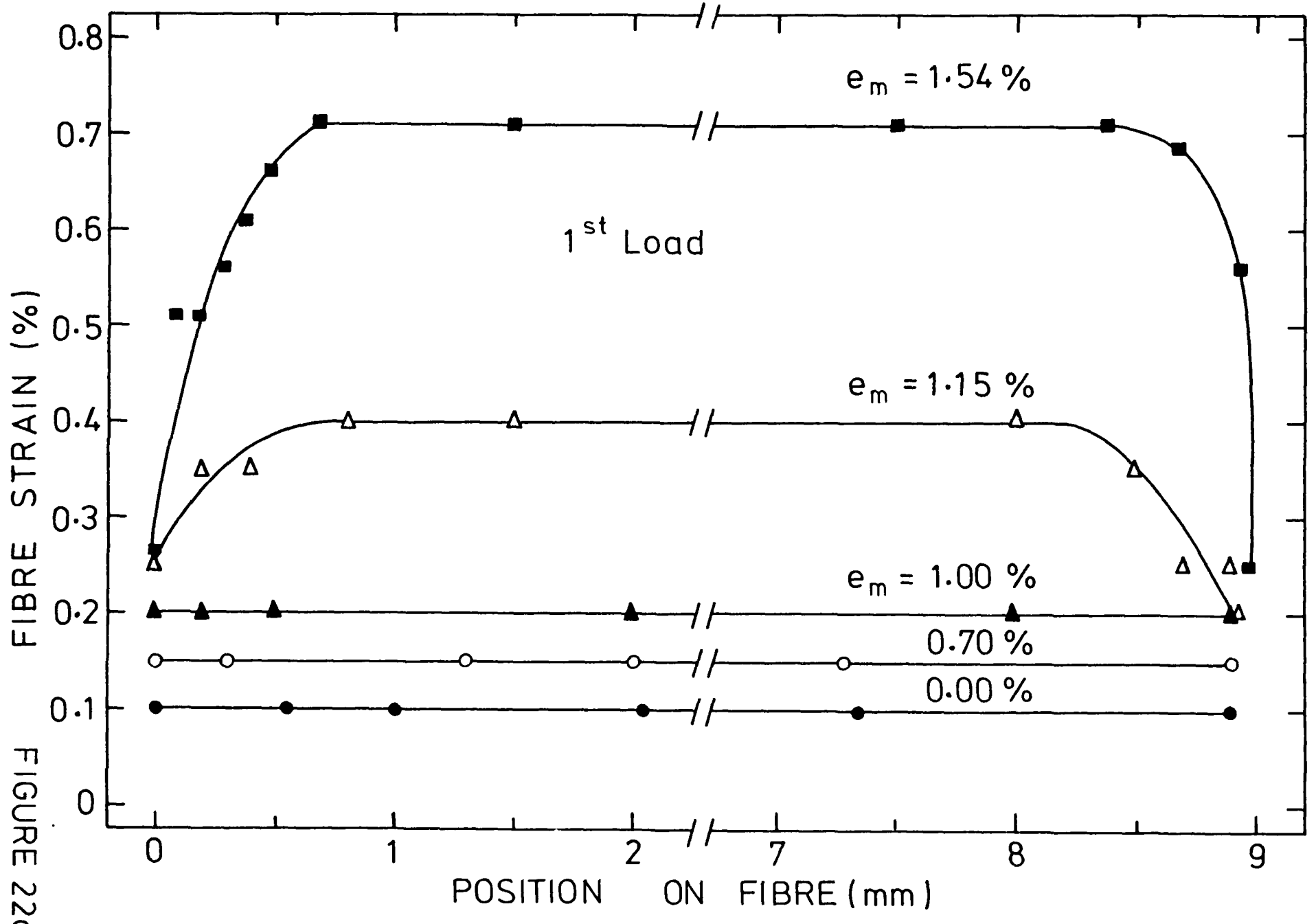
0.8
0.7
0.6
0.5
0.4
0·3
0·2
0.1
0
FIBRE STRAIN (%)
e_m = 1·54 %
1st Load
e_m = 1·15 %
e_m = 1·00 %
0.70 %
0.00 %
0
1
2
7
8
9
POSITION ON FIBRE (mm)

FIGURE 22a

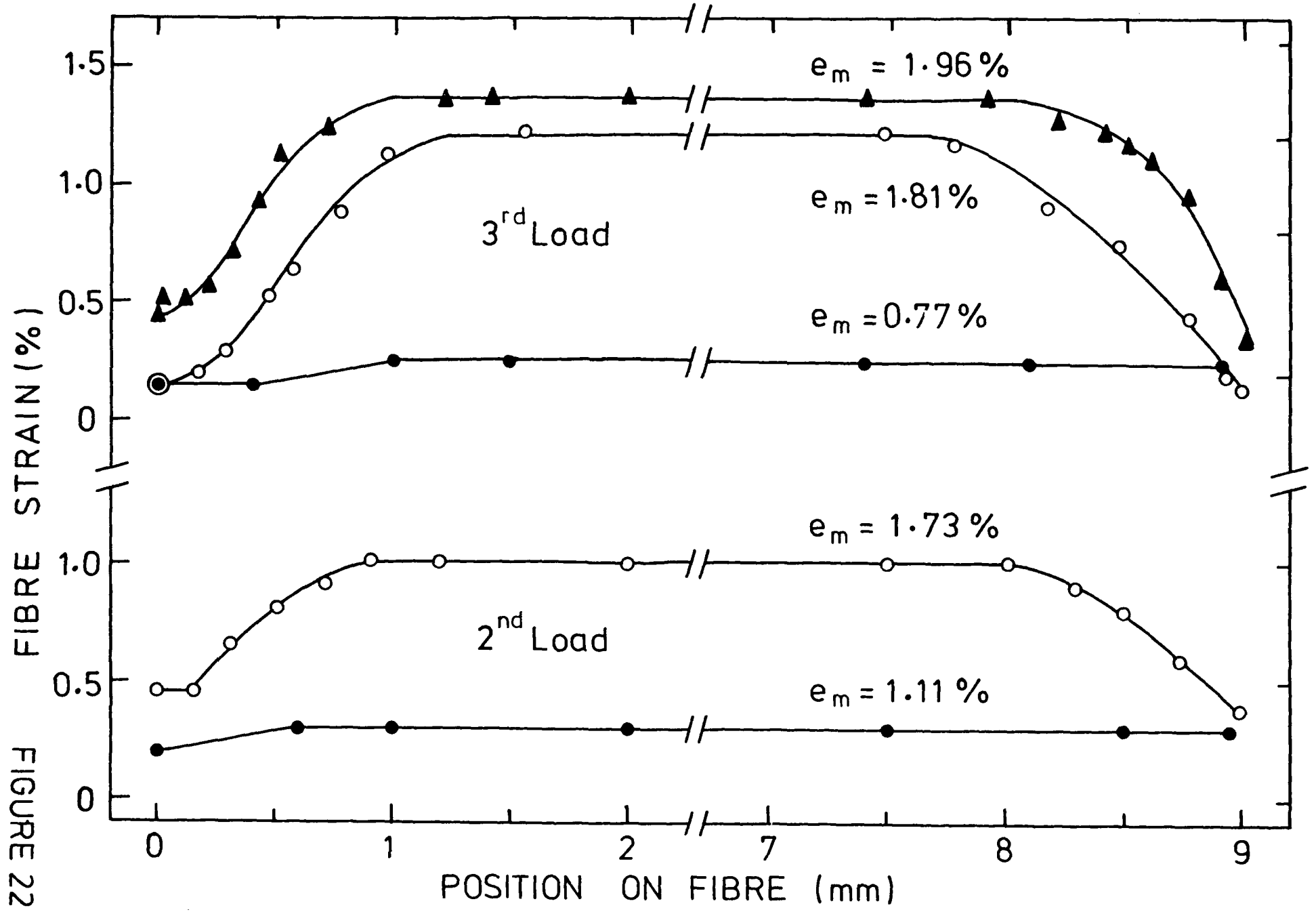
1·5
1·0
0·5
0
e_m = 1·96 %
e_m = 1·81 %
3rd Load
e_m = 0·77 %
e_m = 1·73 %
1·0
0·5
0
2nd Load
e_m = 1·11 %
0
1
2
7
8
9
POSITION ON FIBRE (mm)
FIBRE STRAIN (%)

FIGURE 22b

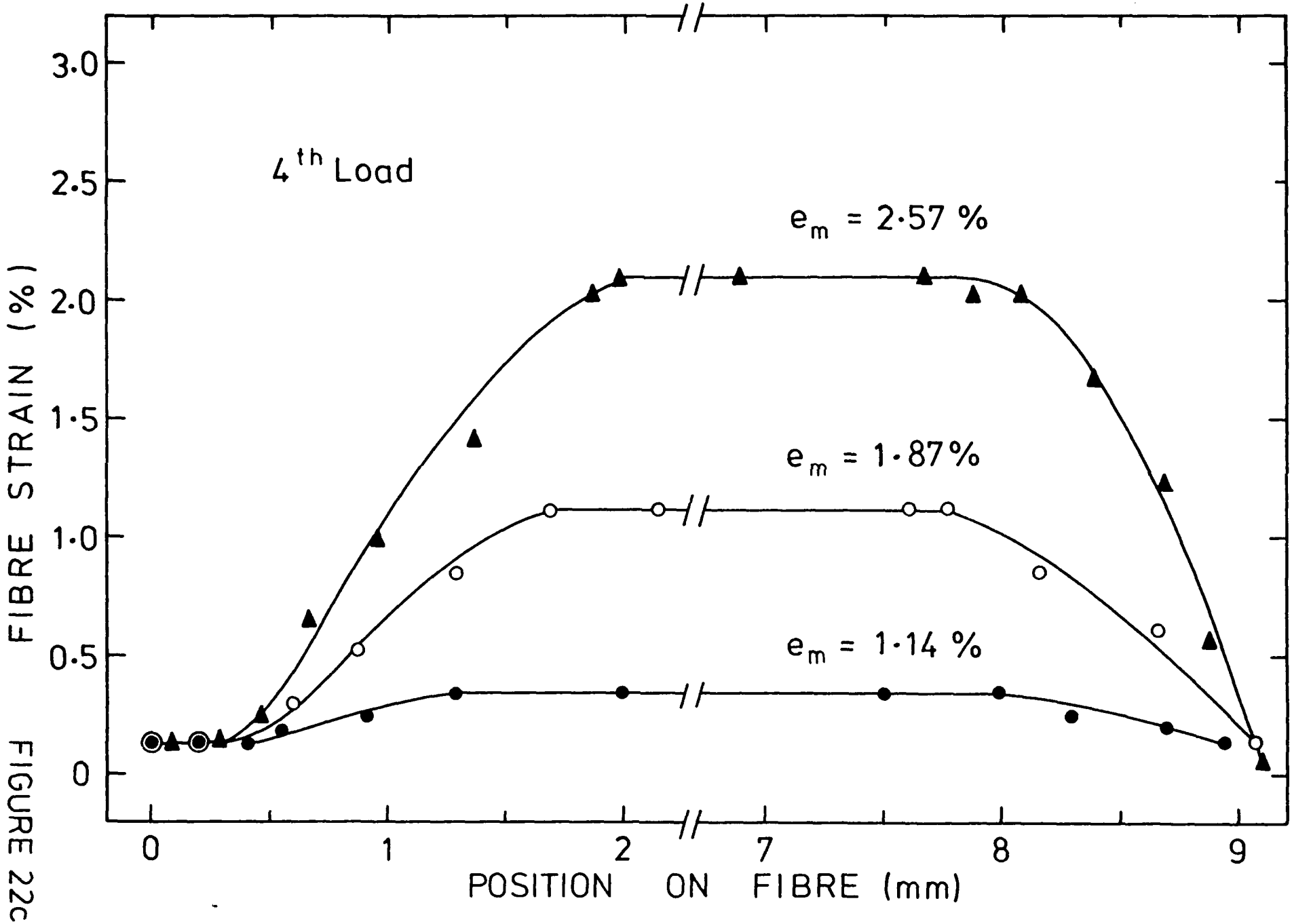
4th Load
e_m = 2·57 %
e_m = 1·87 %
e_m = 1·14 %
FIBRE STRAIN (%)
3·0
2·5
2·0
1·5
1·0
0·5
0
0
1
2
7
8
9
POSITION ON FIBRE (mm)

FIGURE 22c

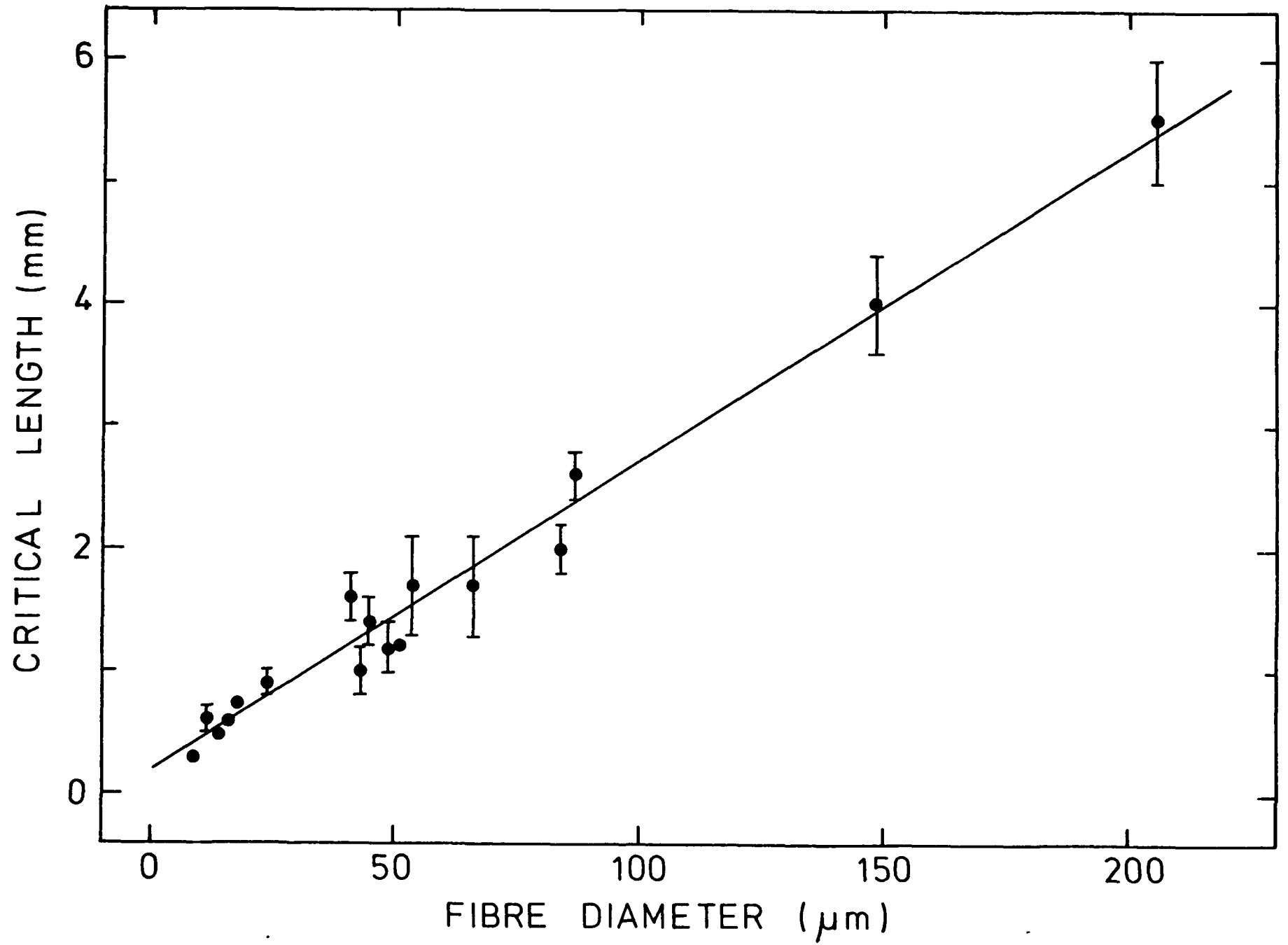

FIGURE 23

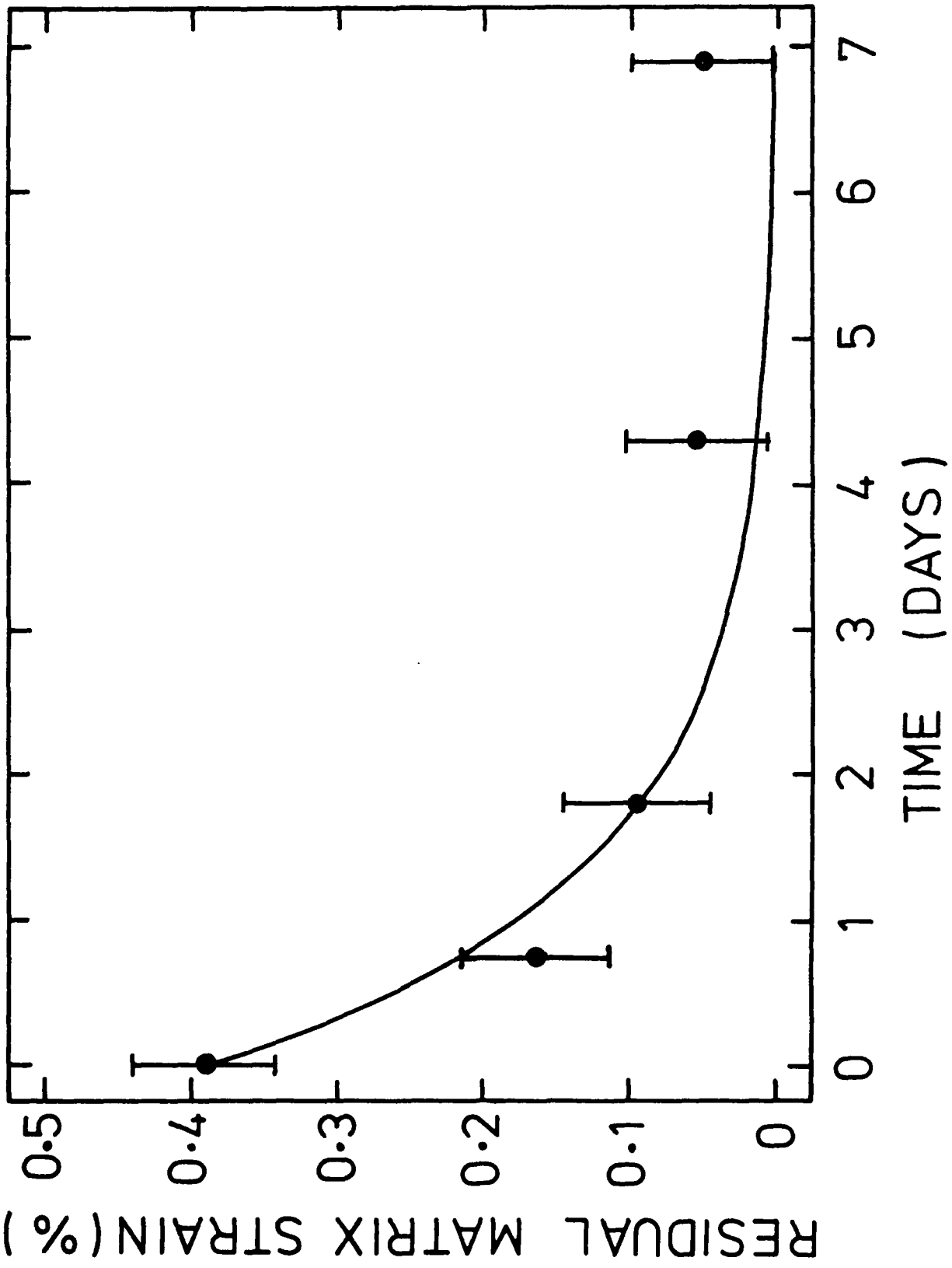

FIGURE 24

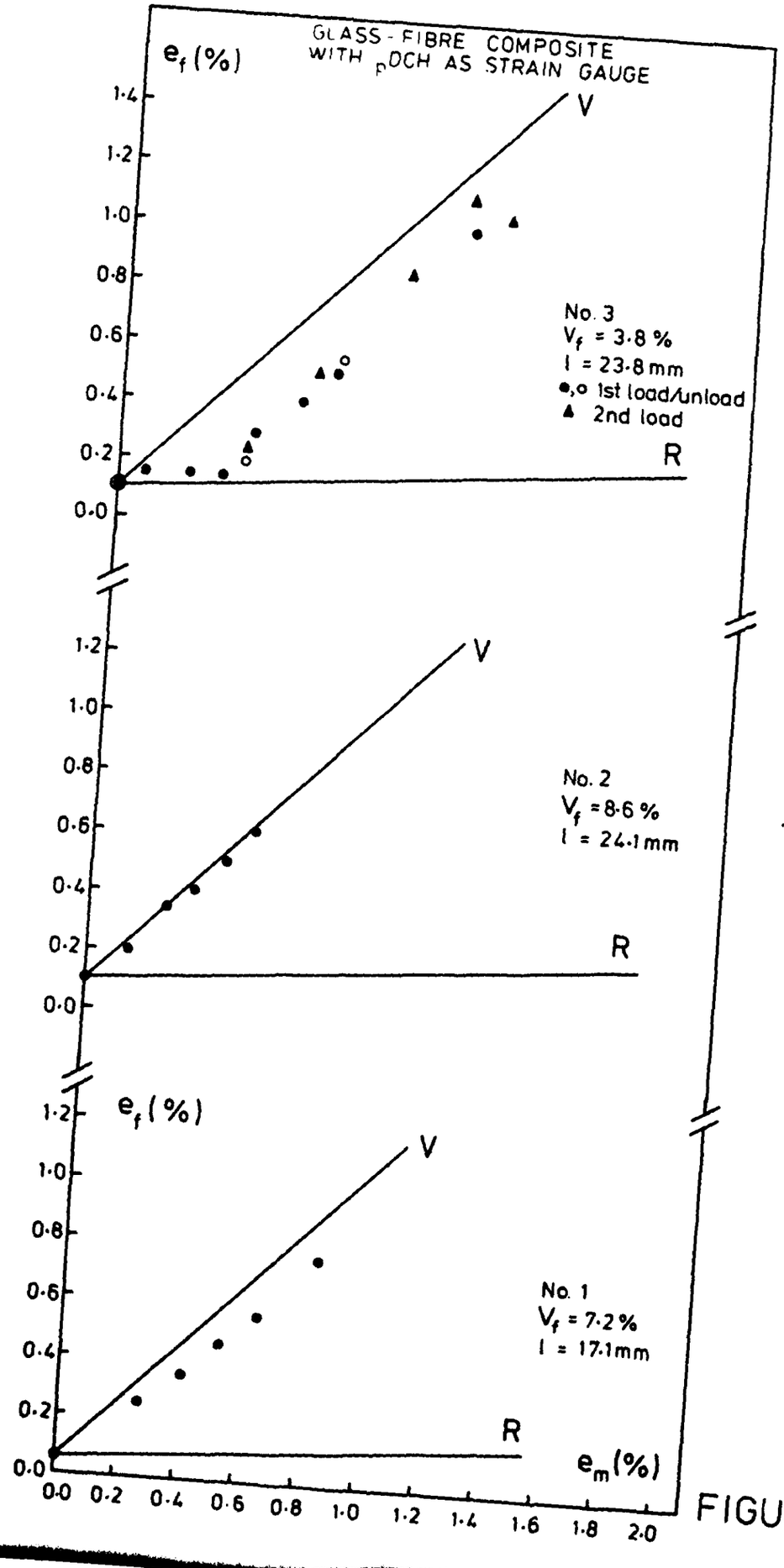
GLASS-FIBRE COMPOSITE
WITH pDCH AS STRAIN GAUGE
e_f (%)
V
R
No. 3
V_f = 3·8 %
l = 23·8 mm
●,○ 1st load/unload
▲ 2nd load
No. 2
V_f = 8·6 %
l = 24·1 mm
No. 1
V_f = 7·2 %
l = 17·1 mm
e_m (%)
0·0 0·2 0·4 0·6 0·8 1·0 1·2 1·4 1·6 1·8 2·0

FIGURE 25

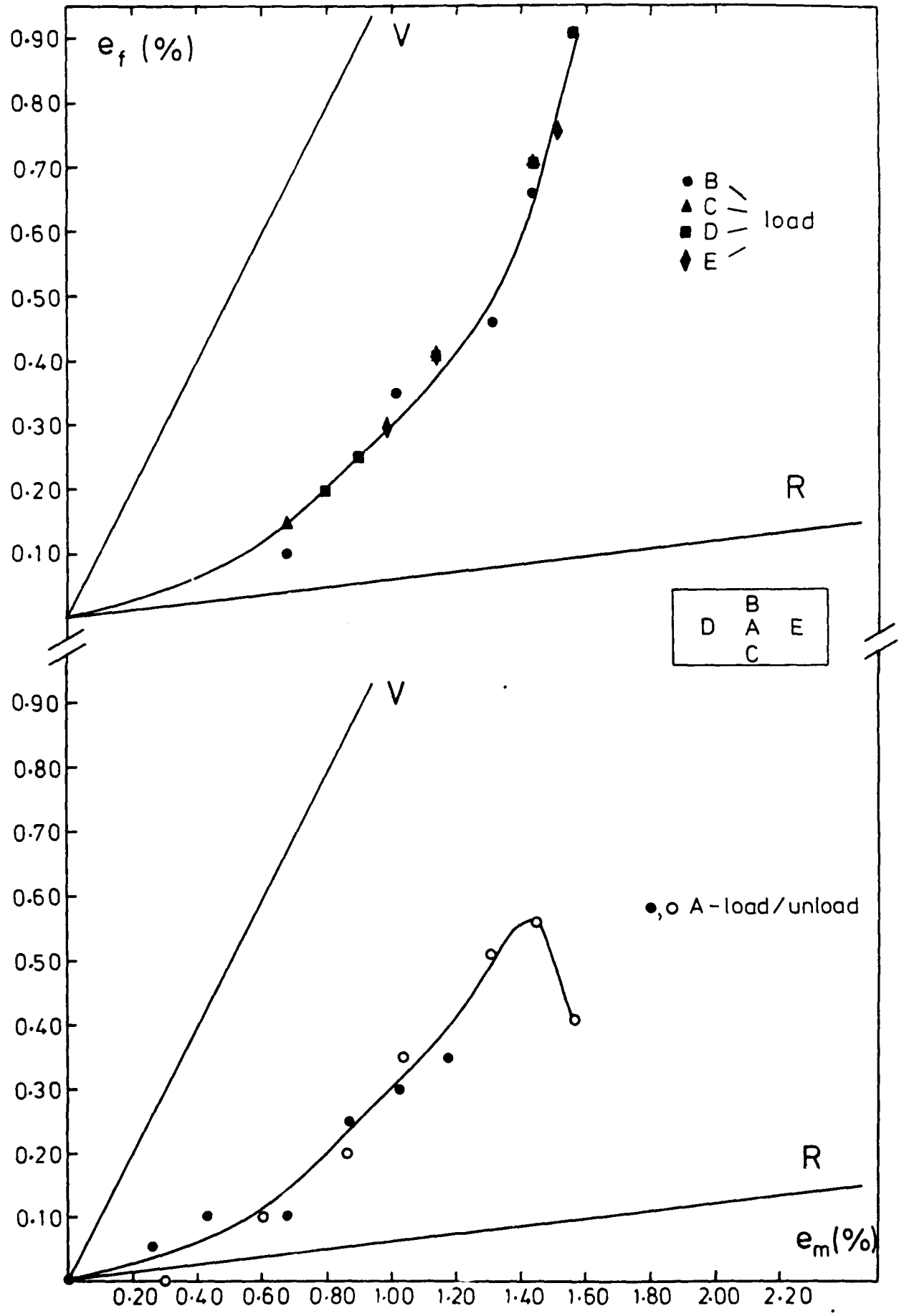
0·90
0·80
0·70
0·60
0·50
0·40
0·30
0·20
0·10
e_f (%)
V
R
B
C
D
E
load
B
D A E
C
V
R
●,o A - load / unload
e_m(%)
0·20 0·40 0·60 0·80 1·00 1·20 1·40 1·60 1·80 2·00 2·20

FIGURE 26

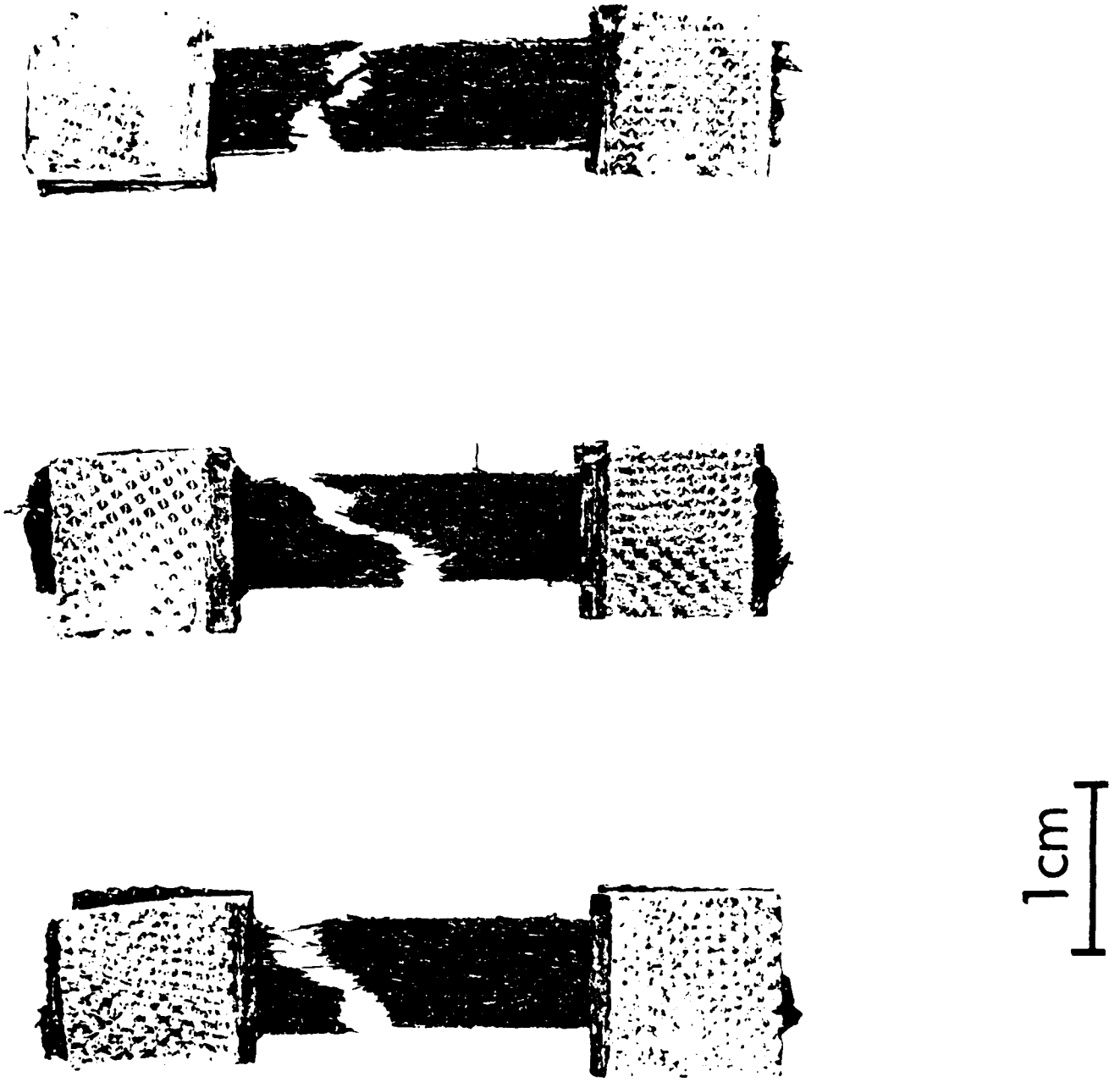

FIGURE 27

FIGURE 28

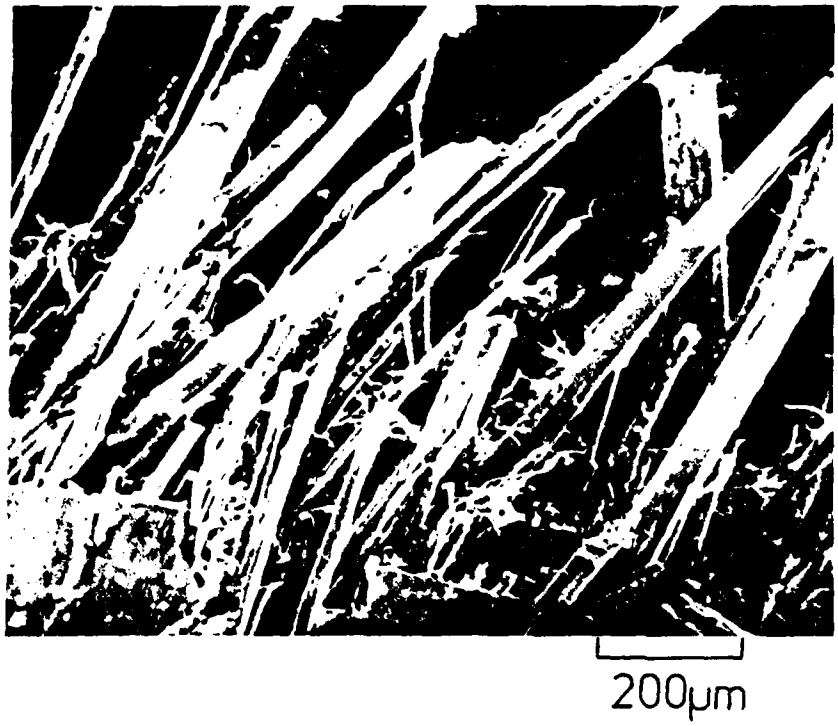

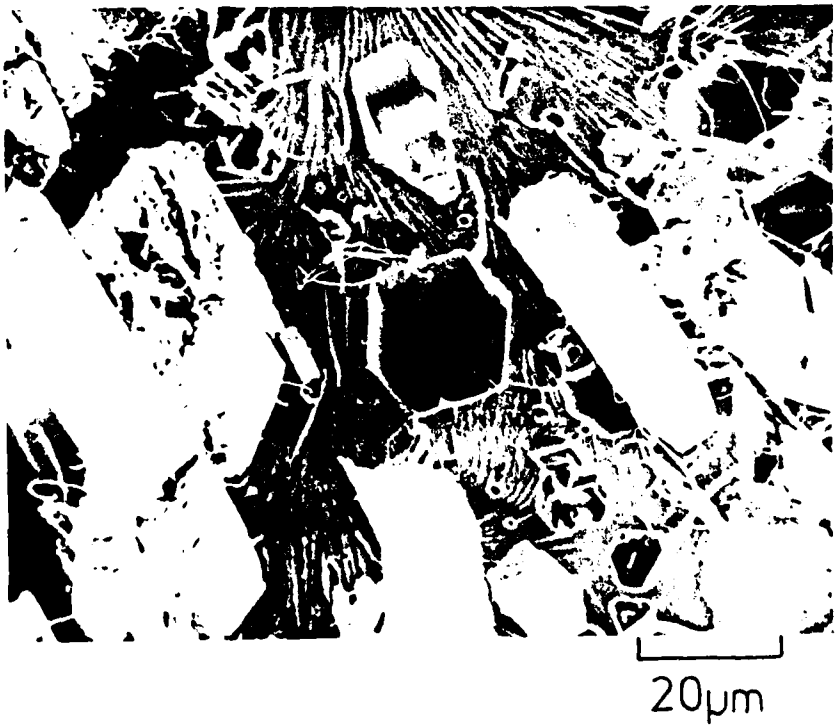

FIGURE 29


DATE
ILME